Particle settling in high viscous pyrolysis char suspensions

Goverdhan Shrestha

Thesis to obtain the Master of Science degree in

Energy Engineering and Management

Supervisors: Prof[a]. Maria Joana Castelo Branco de Assis Teixeira Neiva Correia
Prof. João Carlos Moura Bordado
Dipl.-Ing. Thomas Nicoleit

Examination committee:

Chairperson: Prof. Francisco Manuel da Silva Lemos
Supervisor: Prof[a]. Maria Joana Castelo Branco de Assis Teixeira Neiva Correia
Member of the Committee: Prof[a]. Maria Cristina de Carvalho Silva Fernandes

November 2014

This thesis is based on work conducted within the KIC Inno Energy, in the Msc program Energy Technologies (ENTECH).

The Msc program Energy Technologies (ENTECH) are collaboration of:

Karlsruhe Institute of Technology, Karlsruhe, Germany

Instituto Superior Tecnico, Lisbon, Portugal

Uppsala University, Uppsala, Sweden

Grenoble Institute of Technology, Grenoble, France

This thesis work was carried out at the Institute of Catalysis Research and Technology (IKFT), at Karlsruhe Institute of Technology, Karlsruhe, Germany.

Abstract

At Karlsruhe's bioliq® project, dry lignocellulosic biomass are converted through fast pyrolysis process into a high energy char powder and pyrolysis condensates (organic and aqueous). The char and aqueous condensate are mixed to a suspension known as bio slurry or bio syncrude that has suitable for long time storage and also lead to lower costs for long distance transport.

In the present work, suspensions of char in the aqueous phase obtained in the fast pyrolysis of straw were prepared with the aim of studying the influence of different variables like the char concentration (23.4, 26 and 31.2%), the settling height (150, 84 and 20 cm) and the temperature (20, 35, and 45 ^{0}C) on the settling of the char particles. The result shows that, the settling velocity decreases with the increase of the char concentration in the suspension. However the settling height of the tower does not affect the settling trend of the particles, i.e. the hydrostatic pressure of the suspension does not influence the particle settling. On the other hand, the increase of the temperature from room temperature 20 ^{0}C to 35 ^{0}C and 45 ^{0}C lead to an increase of the particles settling. Therefore, it is possible to conclude that the bioslurry should be stored at lower temperatures. Finally, bioslurry stability was determined using for coal water slurry and stability values of 80 and 79% after 7 days were found for 26 and 31.3% concentration slurries respectively.

Key words: bio slurry, particles settling, concentration, stability

Resumo

No projecto bioliq® de Karlsruhe, a biomassa celulósica é convertida através de um processo de pirólise rápida em coque, com elevado conteúdo energético, numa fase líquida orgânica de elevada viscosidade e numa fase aquosa. Os produtos obtidos depois de misturados dão origem a uma suspensão, o bio-slurry ou bio syncrude, que pode ser armazenada por períodos longos e que apresenta também custos mais reduzidos de transporte a longa distância.

No presente trabalho prepararam-se suspensões de partículas de coque na fase aquosa obtida após pirólise rápida de palha, com o objectivo de estudar a influencia de diferentes variáveis tais como a concentração de partículas na suspensão (23, 26 and 31.3%), a altura da coluna (150, 84 and 20 cm) e a temperatura (20, 35 and 45 ºC), na sedimentação das partículas. Os resultados mostram a velocidade de sedimentação das partículas diminui com o aumento da concentração da suspensão e que a altura de suspensão na torre não afecta a sedimentação ou seja, a pressão hidrostática da suspensão não influencia a sedimentação das partículas. Por outro lado, o aumento da temperatura desde a temperatura ambiente 20 ^{0}C a 35 ^{0}C e 45 ^{0}C levam a um aumento das partículas de decantação. Portanto, é possível concluir que o bioslurry deve ser armazenado a temperaturas mais baixas. Finalmente, a estabildiade do bio-slurry foi determinada utilizando o método estabelecido para coal water slurries, tendo-se obtido valores estabilidade de 80% e 79% após 7 dias para as suspensões contendo 26 e 31.3 % de particulas, respectivamente.

Palavras-chave: bio-slurry, decantação sedimentação das partículas, concentração da suspensão, estabilidade

Acknowledgments

This study was carried out at the Institute of Catalysis Research and Technology (IKFT), at Karlsruhe Institute of Technology, Karlsruhe, Germany. First, I would like to extend words of thanks and acknowledgement towards my supervisors, Dipl.-Ing. Thomas Nicoleit from Institute of Catalysis Research and Technology (IKFT), at Karlsruhe Institute of Technology, Karlsruhe, Germany, Professor Maria Joana Castelo Branco de Assis Teixeira Neiva Correia and Professor João Carlos Moura Bordado from the Department of Chemical Engineering at Instituto Superior Techno, Lisbon, Portugal for their guidance and support throughout this work. I would like to thank the analytical lab colleagues for analyzing the samples. Also, I would wish to convey my greatest gratitude to the people who have helped and supported me throughout my dissertation.

Nomenclature

List of Abbreviations:

BTL: Biomass to Liquid

CNG: Compressed natural gas

CO_2: Carbon dioxide

CO: Carbon monoxide

DME: Dimethylether

FT: Fischer Tropsch

H_2O: water

HCN: Hydrogen cyanide

IBC- Intermediate bulk container

KIT: Karlsruhe institute of technology

L/S: liquid to solid

LPG: Liquefied petroleum gas

NH_3: ammonia

List of Symbols:

ρ_p: density of particle

ρ_f: density of fluid

μ: dynamic viscosity

τ: shear stress

ú: shear rate

dt: change in time

dV_c: settling rate of particles

A: area

Ar: Archimedes number

C: solid concentration

C_d: drag coefficient

C_{max}: maximum concentration

D: diameter of cylinder

d_o: primary particle diameter

d: diameter of particle

g: acceleration due to gravity

J: sedimentation flux

M_I: initial mass of the bio slurry sample

M_N: mass of the non flowing bio slurry

n: exponent empirically related to the particle Reynolds number

Q_p: volume flow rate of particle

Q_l: volume flow rate of liquid

R_p: Reynolds's number

S_{sta}: Static stability

t: time

u: rate of rising of any plane

V: sedimentation velocity of the suspension

V_c: sedimentation velocity of particle

V_l: liquid rise velocity relative to particle settling

V_s: terminal settling velocity

List of Units:

μm: micrometer

%: percent

Cm: centimeter

g: gram

Kg/m^3: kilogram per cubic meter

km: kilometer

min: minute

M/s: meter per second

mm/s: millimeter per second

MJ/kg: mega joule per kilogram

wt.%: weight percentage

rpm: revolution per minute

Table of Contents

List of Figures

List of Tables

1. Introduction

1.1 Motivation

Our world runs on energy. We need energy for every aspect of our life. Society is in a constant struggle to find adequate sources toward growing energy demand because of industrial and economic growth. Last several hundred years; we rely on fossil fuels like coal and oil as our primary resource. These fuels have been in our planet for hundreds and thousands of years. Discovery and use of fossil fuels are unquestionable the fundamental role in building our modern civilizations. At present, more than 80 % of the world's energy consumption is based on fossil fuels [1]. However, this resource is depleted because of the limited reserves and the increasing consumption of energy. With the current consumption trends, world energy demand is estimated to increase by 50% between 2005 and 2030 [2].

The main two largest energy consumers with this increase of energy demand have been the transportation and the industry sector. Traditional liquid fuels developed from fossil resources such as diesel, gasoline, liquefied petroleum gas (LPG) and compressed natural gas (CNG) and play a valuable role in the transportation sector [2]. Currently, more than 90% of the energy used for transportation is derived from petroleum fuels. However, fossil resources are running off, the cost of these fuels is expected to rise and fossils emit huge amounts of greenhouse gases, mainly CO_2 which cause climate changes.

We must start to look for new sources to fulfil our needs. Bio energy, i.e. biomass may be one solution in energy crises. Biomass is not a new discovery, even in fact this have been used before fossil fuels i.e. burning wood is an example of using biomasses. Biomass can be used either directly to heat and electricity or changed into gaseous and liquid fuels with the possibility to utilize more innovative technologies for production of fuels [3].The common first generation bio-fuels, like bio ethanol from sugar containing plants, can be used as a replacement to gasoline. Biodiesel from vegetable oils or animal fats can be used as a replacement for petroleum diesel [4]. However, these bio fuels exhibit high costs mainly due to the limited raw material source. Furthermore, fuel vs. food develops a risk of diverting crop farmland for producing liquid bio-fuels which consequence negatively to the worldwide food supplies [5].

Thus, scientists and industries have begun research on alternative sources for fuel production to make a fuel comparable in cost and efficiency as the fossil fuels and to reduce the fuel vs. food problem. Second generation biofuels derived from lignocellulosic raw materials overcome the problem of raw materials availability. They also offer more variety such as wood, grass, waste materials and much more variety of biomass sources as a feedstock. Biofuels from lignocellulosic materials are mainly produced through thermo-chemical process in the bio refinery. Different thermo-chemical process like pyrolysis, gasification, plasma treatment and liquefaction are used for the production of synthetic liquid fuels or

gaseous fuels. But the design and management of the logistics system for lignocellulosic biomass supply are a critical factor for the development of a bio refinery [6]. It depends on the characteristics and forms of biomass, the location of biomass sources to the bio refinery plant and the mode of transport. And the main disadvantages of integrated bio refinery plant are the high traffic density and the high transport costs for a bulky and low energy density biomass like straw and hay [7]. Due to the low energy density of biomass based on volume, the transportation of biomass is limited to short lengths. This can be only economic if the biomass energy density based on volume significantly increase.

By looking forward to these challenges, Karlsruhe Institute for Technology (KIT) is working on the so called bioliq process: low energy density lignocellulosic biomass is processed by fast pyrolysis to a mixture of pyrolysis condensates and char, a relatively high energy density bioslurry also called bio-syncrude in decentralized or regional plants. This high energy density product is more economical for the transport to the central treatment plant. In central plant, synthesis gas is produced through gasification process and converted to synthetic fuel or other chemical products. For easy transport, loading and unloading, the biosyncrude should be particularly storage stable and pumpable, and therefore the settling of the char particles has to be avoided.

1.2 Objective of work

The bio slurries are stored for a period of time before its use in the gasification process. But it is natural that the particles might settle due to their higher density. Also, depending on the mixing ratio and the characteristics of char and condensates, the slurry tends to build solid sediments. So for storing and transporting it is important, that the slurries remain uniform in solid concentration or the sediments formed in the storage tank be loosely packed so that it can be re-stirred and pumped.

So, the purpose of this work was to characterize the particle settling varying the following variable:

- concentration of the char in the bio slurry.
- height of the settling tower.
- storage temperature.

1.3 The Karlsruhe Bioliq process

The Karlsruhe Institute for Technology (KIT) developed the bioliq process as an example for a biomass to liquid (BTL) fuel production. This allows the conversion of low energy lignocellulosic biomass to high-quality synthetic fuels and other organic chemicals. The concept of bioliq is shown in Figure 1, which approaches two stage processes. As in Figure 1, within a radius of approximately 25 km, the low energy local residual biomass, i.e. straw (2 - 2.5 GJ/m^3) are collected and processed in decentralized plant by fast pyrolysis to produce the high energy bio slurry as an intermediate product. This has an energy density about ten times greater than the original biomass [8]. Therefore, this product can be transported efficiently and economically over long distances to centralized plants. In this central plant, all bio-slurries are collected from different decentralized plants and converted into synthesis gas and finally into high energy synthetic fuels. The concept of decentralized and centralized process plant for converting biomass to liquid is more efficient and economical [8].

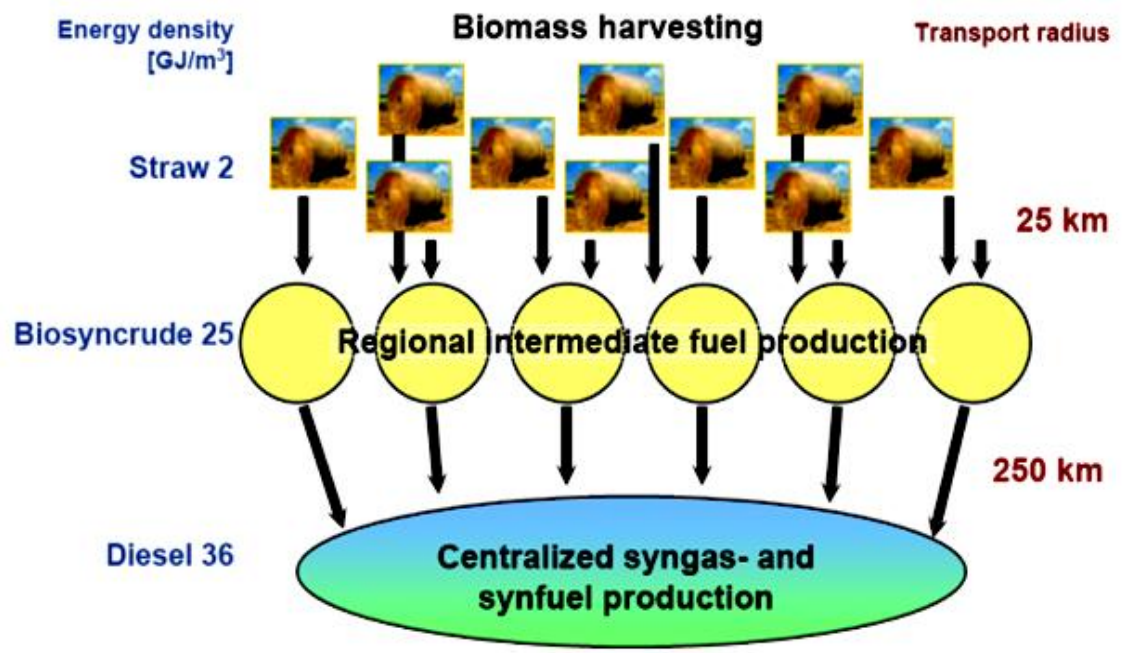

Figure 1: concept of bioliq process [9]

Figure 2 shows the processes of the bioliq project. In the decentralized plant, fast pyrolysis is used in order to thermally decompose dry lignocellulosic biomass at about 500°C in the absence of oxygen. At this temperature, fast decomposition of the biomass yields a maximum of the desired pumpable pyrolysis condensates and lower amounts of pyrolysis char and gas. The char can be completely suspended in about twice as much as pyrolysis condensate to form the bio slurry [7]. In the centralized plant, gasification and gas cleaning of biosyncrude is done to produce the synthesis gas, i.e. mixture of carbon

monoxide (CO) and hydrogen (H_2). Finally the synthesis gas is converted into different fuels or other chemical products, like waxes, methanol, etc. by DME or FT synthesis process.

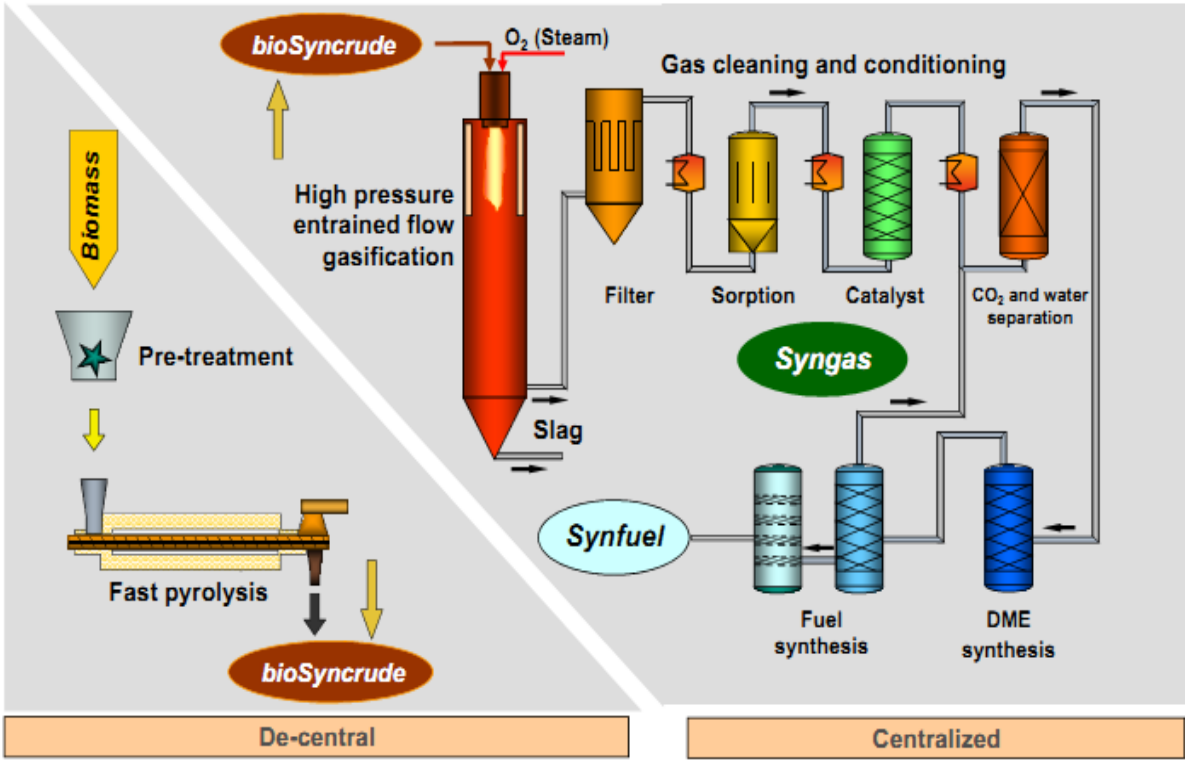

Figure 2: Process stages of bioliq process [10]

Fast Pyrolysis and Bio slurry production

Firstly, the bio condensate and the bio char are generated from the biomass by fast pyrolysis. Regarding the operating parameters of the reactor and the used biomass, 50-70% of condensates and 15-30% pyrolysis char and about 15- 20% gas are obtained. Thus, the main objective of the fast pyrolysis is the production of adequate organic and aqueous liquid for complete char suspension [9]. Fast pyrolysis is conducted in a twin screw mixer reactor heated by a sand heat carrier. In the reactor, biomass are rapidly heated up to approximately 500^0C and thermally decomposed within seconds. Central parts of the fast pyrolysis system are a reactor with twin screws rotating in the same direction, cleaning each other with looping flights and a heat carrier loop. Technically, a pneumatic sand lift has been applied where the heat carrier sand is heated directly by means of burned pyrolysis gas which is generated in the process [11]. The fast pyrolysis process is illustrated in Figure 3.

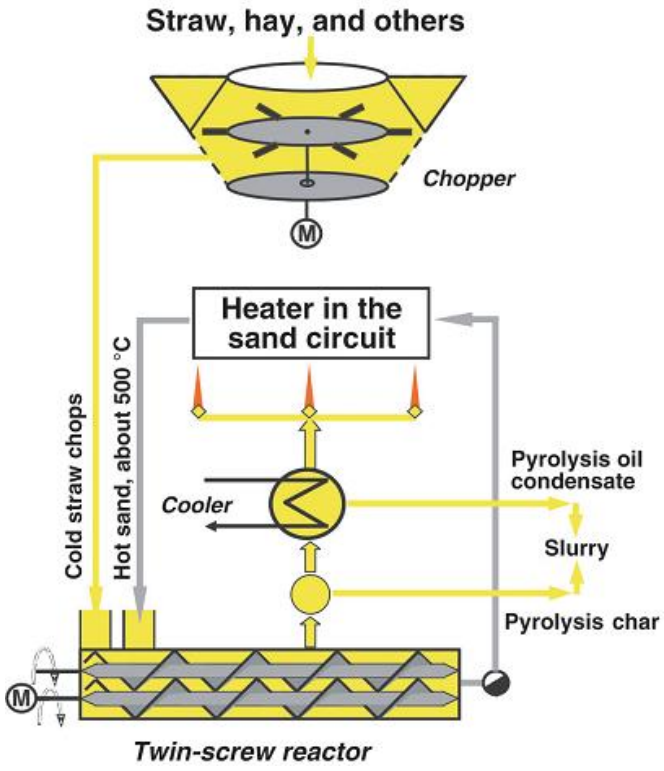

Figure 3: Double screw mixing reactor of fast pyrolysis process [12]

Fast pyrolysis of biomass gives a stream of gaseous, vaporized and solid products. The char is separated from the vapours by a cyclone. The main portion of the vapour is condensed to form liquid pyrolysis products: organic and aqueous condensate. A single step condenser would result in a condensate mixed with organic and aqueous condensate. These condensates are not stable and tend to separate in an organic and aqueous phase. Thus the pyrolysis gases are condensed in two stages. In the initial quench cooler, the organic substances are condensed at a temperature about 110^0C and in the second quench cooler the aqueous condensate is obtained at low temperature of 40^0C.

The char obtained in the bioliq process is a fine powder with the size distribution of 10 -200 μm and high porosity of 50- 80%. The char can be suspended in the organic condensate and in the aqueous condensate. Due to higher heating value of organic condensate i.e. about 20 MJ/kg, it can be used directly into the gasifier. As the heating value of the aqueous condensate is very low i.e. about 4-7 MJ/kg it is better to add the char in order to obtain the highest as possible before gasification process.

Gasification, gas cleaning and synthesis process

The next step is an entrained flow gasification, where the bioslurry is partly reacted with oxygen at high pressure up to 80 bar and temperature more than 1200^0C to form a tar free synthesis gas (H_2, CO) [12]. For the entrained flow gasification, the biomass feedstock needs to be converted into a gas, liquid, slurry

or paste, which can be pumped by a compressor pump into the pressurized chamber. Organic fuel with a higher heating value greater than 10 MJ/Kg can be pumped and atomized in a special nozzle with pressurized oxygen as gasification and atomization agent[10].

Then the crude synthesis gas is purified and conditioned. The gas purification unit removes precipitate particles by means of ceramic filter candles, removes acid gas components and alkalis by means of inorganic adsorbents and catalytically converts NH_3, HCN and organic components in a final catalyst stage. At the last stage of the purification process, CO_2 is removed from synthetic gas by a conventional solvent wash. After purification, the gas converted directly to the DME in a single step synthesis. Then it proceeds to zeolite catalyzed dehydration of DME with oligomerization and isomerization of the hydrocarbon used.

The overall characteristics of bioliq pilot plant are illustrated in Table 1:

Table 1: characteristics of bioliq pilot plant [12]

	Stage 1	Stage 2	Stage 3	Stage 4	Stage 5
Process	Fast pyrolysis	Entrained flow gasification	Gas purification	DME synthesis	Gasoline synthesis
Pressure (BAR)	–	80	80	50	55
Temperature (°C)	500	> 1200	500	250	300
Throughput	500 kg/h of biomass	1000 kg of biosyncrude	700 Nm3/h	50 kg/h	30 kg/h
Product	Biosyncrude	Crude synthesis gas	Pure synthesis gas	DME	Gasoline
	$C_5H_{5.4}O_{1.1}$ + H_2O+ ash	CO+ H_2+ CO_2 + N_2+$(H_2O)_g$ + slag	CO+ H_2+N_2		

2. Literature review

2.1 Biomass and pyrolysis process

2.1.1 Biomass

Biomass is described as “the biodegradable fraction of products, waste and residues from the biological origin from agriculture (including plants and animal), as well as the biodegradable fraction of industrial and municipal waste” [13]. By using various conversion processes such as combustion, gasification, pyrolysis and liquefaction, biomass can be converted into liquid fuels for transportation.

In the pyrolysis process, lignocellulosic biomass consider as a suitable feed stock. The primary components of lignocellulosic biomass are cellulose, hemi-cellulose and lignin, along with the other compounds like acids, salts and minerals in lower amounts [14]. The composition of these components varies depending on the plants. The Table 2 shows the composition of the different lignocellulosic biomass. For example, hardwood contents higher amounts of cellulose, whereas wheat straw has more hemi-cellulose.

Table 2: Composition of lignocellulosic biomass [15]

Lignocellulosic biomass	Cellulose (%)	Hemi-cellulose (%)	Lignin (%)
Hardwood	40-55	24-40	18-25
Softwood	45-50	25-35	25-35
Wheat straw	30	50	15

Cellulose is the important component of lignocellulosic biomass, which is considered as a polymer of glucose. At the temperature between 320-420^{0}C, the cellulose is transformed into organic condensable vapours, char and non-condensable gases [16]. The cellulose yielded the highest amount of organic condensate, and low amount of water and char [17].

Hemi-cellulose is a mixture of various polysaccharides such as glucose, galactose, xylose, mannose and galacturonic acid residues. These components are decomposed at a lower temperature, i.e between 200-260^{0}C [18]. Thus, under higher pyrolysis temperature significant secondary cracking of pyrolysis vapours will ocurrs, which result in higher yields of condensate (with higher amount of water content and less tar), and gas products, and lower amount of char [17], [18].

Lignin is a mostly aromatic polymer consisted mainly of amino acids. It is generally bound to adjacent cellulose and hemi-cellulose fibers to form a lignocellulosic structure. Lignin decompose between the temperature range of 280-500^{0}C [18]. The pyrolysis of lignin yield higher amount of char particles,

moderate range of condensate (with average percent of organic and aqueous fraction), and lower amount of gas product [17], [18].

2.1.2 Energy density of biomass

Utilization of biomass as an energy source has several advantages. But due to some properties, the conversion of biomass into fuel or energy is limited. The energy density of biomass is minimal compared to that of fossil fuels. Furthermore, biomass contain significant amounts of moisture, up to 40-50% by weight. The low density and high water content of biomass makes transportation cost higher. So, there are many traditional technologies to increase the biomass density including baling, cubing and palletizing. In addition, there are different types of thermo chemical process like pyrolysis, liquefaction through which low energy density biomass converted into higher energy density products. Figure 4 shows the relative volume of biomass for wood and straw, intermediate pyrolysis products, and the final mixture (bio slurry). Bio slurry is well suited for energy density storage and transport, resulting in lower transportation costs.

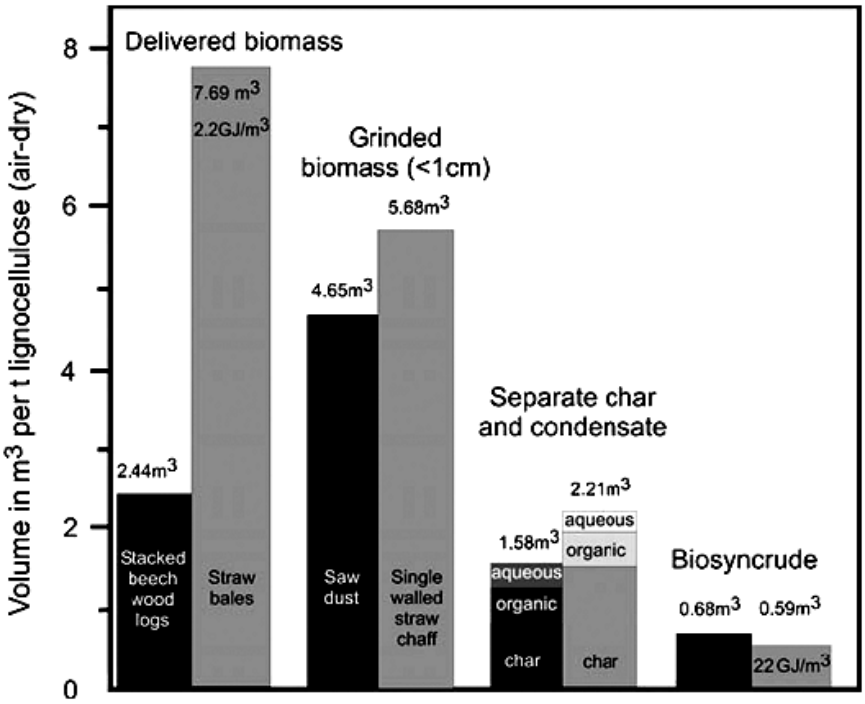

Figure 4: relative volumes of biomass, intermediate products and bio slurry [7]

2.1.3 Yield of fast pyrolysis product

Pyrolysis is the process of thermal decomposition of an organic component in biomass at various temperatures in the absence of oxygen, which results in the production of char and non-condensable gas in slow pyrolysis and additionally condensable vapours (liquid products) in fast pyrolysis.

In the fast or flash pyrolysis process, biomass feedstock is rapidly heated to 450 - 600°C in the absence of oxygen. Under these conditions, vapours, pyrolysis gases and charcoal are produced. The vapours are quickly condensed to pyrolysis condensates, which tend to separate into a bio-oil (organic condensate) and reaction water (aqueous condensate). Typically, 60-75 wt. % of the feedstock is converted to condensates. The product yields of the fast pyrolysis of different biomasses as a reference can be seen in Figure 5. The products char, organic condensate, reaction water, gas is given on a moisture- and ash-free basis.

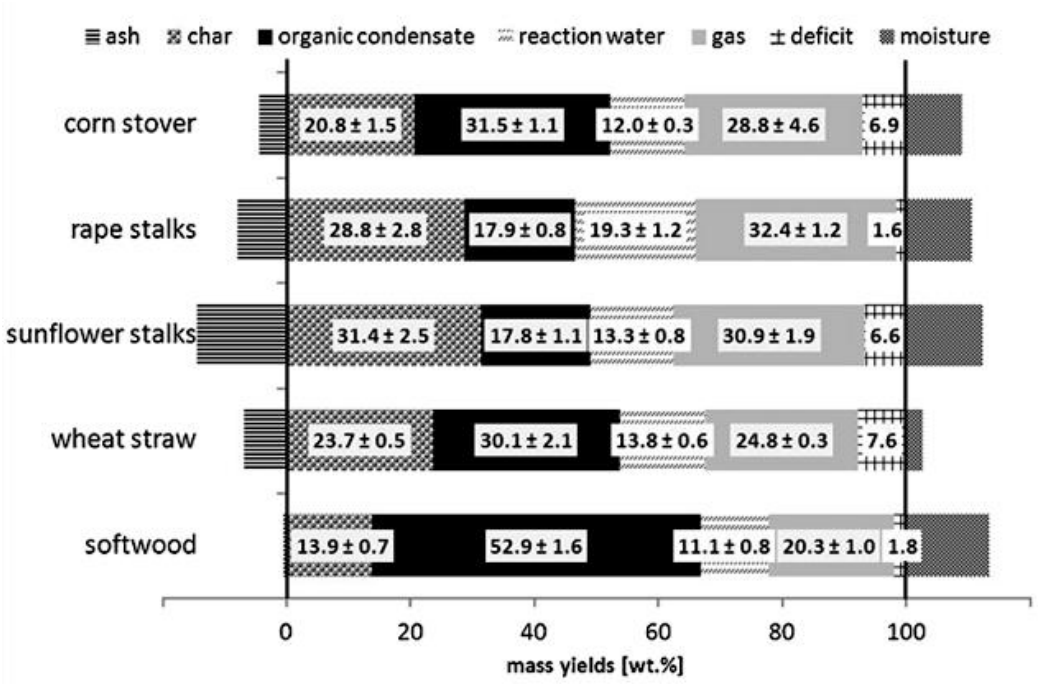

Figure 5: Product yields of different types of biomass [19]

As the organic condensate provides a considerable heating value of about 20 MJ/kg, they can be directly used in gasification. During a fast pyrolysis of straw, around 65 wt. % of char and condensate are produced, which can be mixed to form the bio slurry suspension, whereas woody biomass produces up to 80 wt. % with a much higher condensate to char ratio [19].

2.2 Slurry mixing technology

To produce slurries, finely ground char, biomass or coal particles are suspended into organic (bio oil) or aqueous liquids. These technologies are designed to improve the transportability of the pyrolysis products and increase energy density, as char or coal powders have low densities due to high porosity. Important slurry characteristics are the stability, pumpability, atomizability and combustion characteristics [20]. Particle concentration and the particle size distribution are considered as important hydraulic variables in

the slurry preparation [21]. Typical slurry production involves preparation, storage, transportation and end user applications, which is in this case the entrained flow gasifier.

If the pyrolysis products are examined individually, the bio oil may need to be further upgraded and refined for the production of liquid transport fuels Depending on the water content, the pyrolysis condensates have a high volumetric energy density and are favourable for transport [22]. The bio char is also a quality energy carrier, which can be used for co-firing in coal fired plant due to its good grindability and the significant specific energy densification. But due to the possibility of spontaneous combustion, long time storage is not favourable. The energy density and therefore the transportability are enhanced by suspending the bio char in the bio oil respectively the aqueous condensates to produce bio slurry as energy carrier.

As the particles have a higher density, they might settle down. Hence, it is important that the slurries in storage tanks remain with uniform solids concentration, or at least remain pumpable while being stored. Loosely packed sediments are suitable, as long as they can be re-suspended by agitation.

Pyrolysis chars have a high porosity between about 50 to 80%. So during the mixing, the pores first soak up much liquid until a sufficient volume remains as lubricant outside the particles as showed in Figure 6. The liquid to solid (L/S) volume ratio, i.e. corresponds to condensate-to-char weight ratio should be 2 to 3:1, which is usually sufficient to prepare free flowing slurries after warming and colloid mixing. If the char concentration exceeds the sedimentation density as an L/S weight ratio below about 2, pastes or sludge are obtained. Pumpable slurries of nonporous coal and water with L/S weight ratio of about 0.4 have been in practice [10].

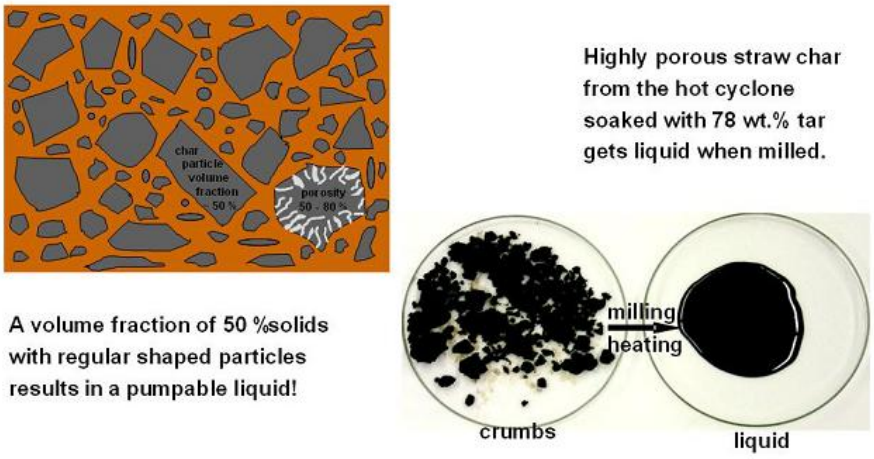

Figure 6: principle of slurry preparation [10]

Abdullah, Mourant, Li and Wu [23] present fuel and rheological properties of bio slurries, made with bio oils and pyrolysis chars. They found that the bio slurry has a high volumetric energy densification and

meets the requirements for the combustion and gasification process. Thus, this bioslurry can potentially replace the conventional fuel use in energy plants, or particularly applications like boilers and gasifier.

Natarjan and Suppes [24] investigated the effects of concentration of corn starch on slurry stability, rheology and viscosity. The mixture with 40% corn starch and 0.15% polyacrylic has favourable rheological property (i.e. lower viscosity at high shear stress) for injection and pumping and also for slurry stability. The settling of corn starch particles didn't occur over a 2 month period.

Benter, Gilmour and Arnoux [25] studied the production of slurries from ground biomass with diesel and kerosene. They concluded that the settling of wood particles can be stopped by emulsifying the slurry mixture with the polar liquid like water and/or ethanol. The slurry of 20% ground wood in kerosene with adding water and ethanol from 15 to 20% produce stable suspension for more than 30 days without any additional additives. They conducted an experiment with various additives in which addition of rheocin is found a more suitable stabilizer for enhancing the stability of the slurry mixture.

He, Park and Norbeck [26] published rheological properties of coal water slurries, biomass water slurries and merged biomass and coal water slurries. They also considered the effects of hydrothermal pre-treatment processes to increase the solid concentration. The slurry pumpability decreases with increasing solid concentration respectively viscosity. But with the hydrothermal processing, the solid concentration can be enhanced maintaining the same viscosity. Thus, the solid concentration of biomass water slurry could be increased from 12.5% to 35%, while maintaining the viscosity less than 700 mPa.s. In the merged biomass and coal water slurry, concentrations of up to 45% could be reached.

Winkeler, Bassin, Kleerebezem and Loosdrecht [27] present the temperature effect on settling velocity in water-based granular sludge. In this study, they showed that the temperature dependent density and viscosity changes of water have great impact on settling velocity of granular sludge.

Ugwa, Ofomatah and Eze [28], studies on Coal–water slurries were prepared with a sub-bituminous coal at varying coal and water ratios using an anionic liquid soap as a surfactant. The slurry properties like viscosity and stability were determined. The rheological properties of the slurries were investigated to determine the characteristics of the slurries. The results showed that increasing coal (solid) concentration increased the density of the slurries, which led to more viscous slurries. The behaviour of the slurries changed from Newtonian to non-Newtonian at higher solid concentrations. The slurries with lower solid concentration settled faster than the higher concentrated slurries.

2.3 Particle settling

Settling is the process, whereby particles in suspension settle out of a fluid and build a concentrated sludge or sediment at the bottom. After this process, the suspension is separated into two phases: clarified liquid on the top of the settling tank and concentrated sludge in the bottom of the settling tank.

This is natural, when the dispersed particles have a specific gravity greater than that of dispersing medium: the particles tend to settle down by gravity or centrifugal motion in the direction exerted by that force. The stability of the suspension depends on the densities of dispersed particle and dispersion medium, the viscosity of the medium, surface properties of particles and other parameters.

2.3.1 Type of settling

For the low concentration slurry, settling takes place freely following the Stokes equation [29], as in equation 1. But for the concentrated slurry, the settling becomes a complex process. Also interactions between the particles form flocs or coagula. So, according to the particles present in the suspension, the settling can be defined as; discrete, flocculent, hindered settling, or compressive settling.

- **Discrete or free particle settling:**

The particles do not interact with adjacent particles and they settle separately in a gravitational field. In this type of settling, coarse particles settle at the bottom, whereas the finest particles remain on the top, if the gravitational forces are not strong enough to overcome frictional forces.

- **Flocculent Particles Settling:**

Individual particles stick together and form loose, porous clumps called flocs. This takes place, when there is a higher solid concentration and/or chemical reaction influences the particle surfaces to enhance attachments. The flocs settle relatively slow due to additional drag forces which formed from these flocs, filling a large fraction of the original slurry volume. Also the loose structure of the flocs contains a considerable amount of entrapped liquid, leading to a relatively lower density difference. Thus, the volume of the final sediment is relatively large and it can be re-dispersed by mechanical agitation. Further compaction of the flocs is only possible by the breaking of the floc bonds and the squeezing out of the liquid through the surrounding particles.

- **Hindered particle Settling:**

If the concentration of particles in a suspension is increased, individual particles stick together and form a compact and tightly bound cluster known as coagulated. These clusters tend to settle as a unit and there is also a net upward flow of liquid, which is displaced by the settling clusters, which leads again to a lower settling velocity. Formed sediments might be compact and difficult to re-disperse or break. In these types of settling, it is possible to make a distinction between various distinct zones, divided by concentration discontinuities. So this is termed as “zone settling“ (see also section 2.4.).

- **Compression settling:**

With the highest particle concentration, the settling can occur through compaction of the structure, and so it takes place at a reducing rate. This is termed compression settling. If the compression settling takes place, settled particles are compressed under the weight of overlying particles, the pore spaces are gradually decreased and liquid is driven out of the pores.

2.3.2 Settling velocity equations

The settling can be seen as differential motion among particles of different size, density with relative to the medium. During this process, flocculation or hindered settling can occur. This is due to complex interactions between particles and fluid, whose separation is based on the settling rates of particles. For this, an equation for velocities of falling particles in a liquid suspension is required for different size of particles. In a free settling, this is comparatively simple to determine, using Stokes or Newton's law depending upon the Reynolds number.

Particle settling is controlled by three external forces: gravity force due to the gravitational field, buoyancy force due to the displacement of the fluid by the particle and the friction force due to relative motion of the particle and the fluid [30]. These forces are a function of particle properties like size, shape, density and fluid properties like density and viscosity. As a function of the settling time, the forces reach an equilibrium point in which the gravity force is balanced by buoyant force and drag forces. From this point, the particles move at a constant maximum velocity; this is known as settling velocity.

The settling rate in higher concentration systems is influenced by particle collisions, hydrodynamic interaction and any forces which may reside on the surface of the particle [31]. The higher concentration of particles in suspension caused the hindered type of settling and the settling rate is defined as the hindered settling velocity. The hindered settling velocity is the strong function of concentration. Different models have been developed to established relationship between hindered settling velocity of suspension and concentration of suspended particles (Richardson and Zaki [32], Concha and Almendra [33]).

- **Particle settling according to Stokes law**

Particle settling velocity of spherical particles for a free settling is given by;

$$V_s = \frac{(\rho_p - \rho_f)\, g\, d^2}{18\, \mu} \qquad \text{Equation 1}$$

where, V_s is the settling velocity, g is gravitational acceleration, d is the particle diameter, ρ_p is particle density ρ_f is the fluid density and μ the dynamic viscosity [30]. This equation implies for the region where the particle Reynolds number (R_P) is less than 1.

$$R_p = \frac{V_s\, d}{\nu}$$ Equation 2

Where ν is the kinematic viscosity.

For the higher R_p, empirical solution is necessary to calculate the drag forces. One such solution is given by Schiller and Nauman which is valid for Rp< 800 [30].

$$C_d = \frac{24\,(1 + 0.15\,R_p 0.687)}{R_p}$$ Equation 3

- **Hindered settling velocity of a particle**

To correlate the hindered settling rate of the suspension with the volume fraction of solids (C) Richardson and Zaki's provide hindered settling correlation [32], given by :

$$V = V_s(1 - C)^n$$ Equation 4

Where, V is the sedimentation velocity of the suspension, V_s is the settling velocity of the single particle and n is the exponent empirically related to the particle Reynolds number (R_P). Volume fraction of solids (C) is equal to volume of particles by the total volume of suspension.

The sedimentation velocity of the suspension is the difference between the settling velocities of particles and the liquid rise velocity relative to the particle settling. This is given by:

$$V = V_c - V_l$$ Equation 5

The different relation is given for index n according to the particle Reynolds number:

$$n = 4.65 + 19.5\,\frac{d}{D} \qquad \text{for } R_p < 0.2$$ Equation 6

$$n = 4.36 + 17.6\,\frac{d}{D}\,R_p^{-0.03} \quad \text{for } 0.2 < R_p < 1$$ Equation 7

$$n = 4.45\,R_p^{-0.1} \qquad \text{for } 1 < R_p < 500$$ Equation 8

$$n = 2.39 \qquad \text{for } 500 < R_p < 7000$$ Equation 9

Where, d/D is the particle to cylinder diameter ratio. For Reynolds number in the Stokes flow region and negligible wall affect the value of n is given as 4.65 for spherical particles. The parameter n is a function of Reynolds number, but not a function of particle to wall diameter ratio. By Khan and Richardson proposed relation of n relates to the Archimedes number (Ar) given by[34]:

$$n = \frac{4.8 + 0.103\ Ar^{0.57}}{1 + 0.043\ Ar^{0.57}}$$ Equation 10

Where, Ar is given by:

$$Ar = \frac{d^3\ \rho_f\ (\rho_p\ - \rho_f)\ g}{\mu^2}$$ Equation 11

Wallis suggested determining the index n by the approximation[35].

$$n = \frac{4.7\ (1 + 0.15\ R_p{}^{0.687})}{(1 + 0.15\ R_p{}^{0.687})}$$ Equation 12

Which cover all range of R_p

2.3.3 Method for sedimentation analysis

Based on different combinations of the force field, the level of measurement in the suspension and the dispersion of particles at the start of the measurement, there are different methods for sedimentation analysis. According to the position of particles at the beginning of the measurement, there are "homogeneous methods", where particles are uniformly distributed and "line start methods" where particles at the beginning are concentrated in a thin layer up the top of the solid free medium. Depending on the place of quantity measurement in the suspension, there is the "incremental method", where the concentration of solids in a thin suspension layer is measured in knowing height and time. With the "cumulative method", the rate of solids settle out of suspension is measured. There are measurements based on particle mass, such as the sedimentation balance method, decanting method and pipette method; measurement based on suspension density, such as the method using manometers, aerometer or various divers and measurements based on the electromagnetic radiation such as light attenuation, scattering of γ-radiation, of light or x-rays and backscattering of β-radiation [36] [37].

Li, Lou and Qiu [38] studied the stability of coal water slurry and sedimentation behavior of particles with the dispersion stability analyzer and concluded that the analyzer provides more accurate data than traditional methods. This analyzer provides more applications like to analyse the stability of the slurry with observing the stability mechanism of slurries.

2.4 Batch sedimentation or zone settling

If there is no adding or remove of the slurry during the sedimentation, the process is called batch sedimentation, whereas, if the solids are steadily removed, the process is called continuous thickening.

In batch processing, initially the sedimentation tower contains a homogenous mixture. Figure 7 represents a typical batch settling column test on a suspension showing zone settling characteristics. As the settling takes place, at the top of the tower a clear liquid interface is formed (A). As the particles settle

down, a uniform concentration zone (B) and a non-uniform zone (C) is formed. At the bottom, solid particle compressed and formed stronger sediment (D) with the increasing storage time.

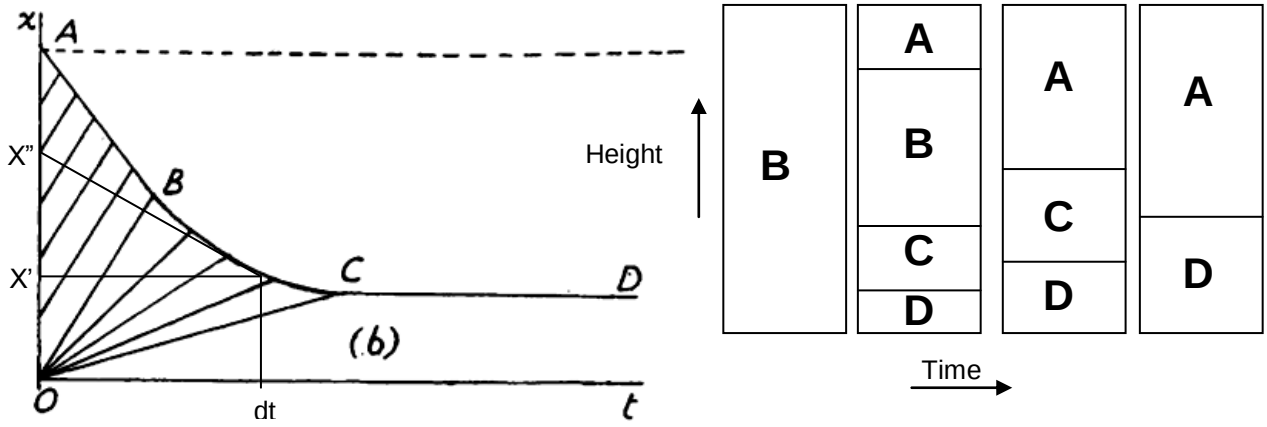

Figure 7: Zone settling behaviour in typical batch sedimentation [39]

A: clear liquid, B: uniform mixture, C: non uniform mixture, D: sediment

t:time, x: suspension height, x": interface height at certain time, x': final interface height at dt

In Figure 7, initially, the suspension settles at a constant rate in the section A to B, and if the particles become of fairly uniform size, sharp discontinuities form between these layers. Between the regions B and C there may or may not be distinct continuity. As the time increases, the upper discontinuity meets the lower and the region B disappears. Then a gradual compression of the regions C and D occurs until finally the sediment formed. The slope of the settling curve at any point represents the settling velocity of the interface between the suspension and the clear liquid.

Since there is no net flow through the tower, the continuity equation is given by:

$$Q_p + Q_l = 0 \qquad \text{Equation 13}$$

Where, Q_p is the volume flow rate of particle settling is given by: $Q_p = V_c A C$

and Q_l is the volume flow rate of liquid moving upwards is given by: $Q_l = V_l A (1 - C)$

Thus the velocity of liquid can be calculated by:

$$V_l = -\frac{V_c C}{(1 - C)} \qquad \text{Equation 14}$$

This type of settling has been analyzed by Kynch (1952) [39]. His analysis is based on the assumptions that the settling velocity of particles V_c is a function only of the local concentration (C) of particles and the settling velocity tends to decrease as the concentration approaches a limiting value corresponding to that of the sediment layer deposited at the bottom of the settling column.

The volumetric rate of sedimentation per unit area or flux (J) is given by:

$$J = C V_c \qquad \text{Equation 15}$$

Two layers at height x and x+dx within the transition zone are considered as shown in Figure 8, having a suspension concentration C. On its upper layer, there is a layer of lesser concentration and on its lower layer there will be a layer of higher concentration. By the time dt the position of this layer moves upward with the rate of u and settling rate of particles decrease by dV_c.

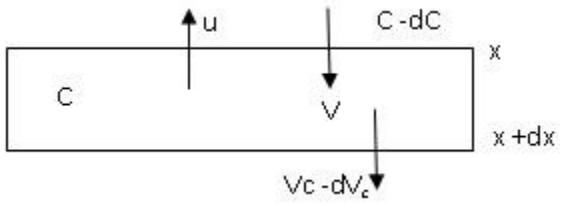

Figure 8: Kynch settling behaviour

Since the concentration within the layer between x and x+dx remains constant, the influx of particles through the upper layer must be equal to the out flux of particles through the lower layer.

$$(C - dC)\,(V_c + u) = C\,(V_c - dV + u)$$

We get,

$$u = -V_c + \frac{dV_c}{dC} \qquad \text{Equation 16}$$

Since V_c is a function of C and assume as constant, thus the rate of rising of any plane of fixed concentration is constant i.e. u = constant =dx/dt. In a uniform suspension of concentration C, the interface between the suspension and the liquid will fall at a constant rate until a zone of composition greater than C, has propagated from the bottom of the free surface. The sedimentation rate will then fall off as a zone of higher concentration reaches the surface, until sedimentation will stop when the C_{max} zone reaches the surface.

The relation between V_c and C can be obtained from a batch settling test. In the beginning at time t=0 the suspension has uniform concentration C and at initial height x. Over time t= t' the interface has dropped to a height x" and the new concentration is a C'. The total mass of solid in the column at t=o, is given by CxA, where A is the cross section area of the column. At time, t=dt the total mass will have to pass through the plane of concentration C' as it moved up from the base of the column with velocity u. This is given by:

$$C \times A = C' (V_c + u) A \, dt \qquad \text{Equation 17}$$

Thus the velocity of ascent is constant and therefore equal to dx"/dt, we get:

$$C \ x = C' (V_c + \frac{x''}{dt}) \, dt \qquad \text{Equation 18}$$

The settling velocity of the particle is given by the slope of the settling curve at (x', dt) and from Figure 7 by drawing a tangent to the curve at this point the slope is equal to -(x" – x')/dt . Thus we obtain:

$$C' = C \frac{x}{x'} \qquad \text{Equation 19}$$

Therefore, in batch settling test the settling velocity for any given concentration can be obtained and the concentration at the interface can be determined.

2.5 Rheology

Rheology is the survey of the flow of matter; liquid or solid under conditions in which they flow rather than deform elastically. This also applies to substances with a complex structure like: mud, slurry, suspensions, and polymer materials. Fluid behaviour is shown in Figure 10. Two extreme of rheological behaviour are:

Newtonian or Viscous behaviour: any deformation that ceases when the applied force is removed. The viscosity is constant with changing shear rates, i.e. the relation between the shear stress and shear rate is linear passing through the origin. Simple Newtonian behaviour is given by;

$$\text{Viscosity } (\mu) = \frac{\text{shear stress } (\tau)}{\text{shear rate } (\acute{u})} \qquad \text{Equation 20}$$

Non- Newtonian behaviour: viscosity of non Newtonian fluid is dependent of shear rate. The relation between the shear stress and the shear rate is not linear, i.e. shear stress change with the shear rate. This type of fluid behaviour is found common in coal water slurry, coal algae slurry, coal oil mixture, coal biomass slurry, sludge slurry, and bio char slurry [40],[41],[42],[28], [43]

Types of Non- Newtonian behaviour

- **Time independent viscosity**

This type of flow behaviour is not affected by the length of time that the fluid has been flowing.

Pseudo-plastic or shear thinning: structures and the viscosity changes with the force. Molecules or particles are arranged in order pattern. The viscosity of pseudo-plastic fluids decreases with the increased shear rate as shown in Figure 10.

Dilatant or shear thickening: resists distortion more than in proportion to the applied force. Molecules or particles are arranged in disordered pattern. For dilatant fluids, the viscosity increases with increased in share rate as shown in Figure 10.

- **Time dependent viscosity**

When viscosity at a given shear depends on time, the systems are;

Thixotropic: with increasing time of applied force to cause a viscosity reduction. The applied force could be agitating, shaking or pumping. These forces help to disperse the coagulated formed in the suspension as in Figure 9. This effect is sometimes known as “work softening”. This process is reversible; if the applied force is stopped, then thixotropic slurry/ fluid regains its viscosity.

Rheopectic: material becomes more viscous with increasing time of applied force. This effect is known “work hardening”.

Time dependent effects are significant; curves measured by increasing shear do not coincide with curves measured by decreasing shear as in Figure 10. Also, these effects are caused by the breaking or building of structures within the flowing matter.

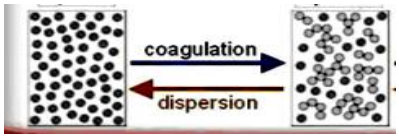

Figure 9: time dependent effect

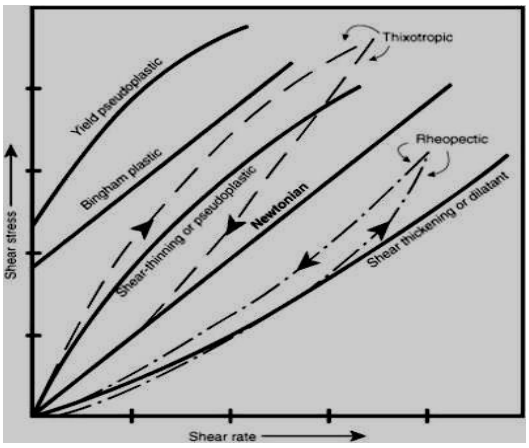

Figure 10: Fluid flow behaviour

3. Materials and Methods

3.1 Materials and its properties

3.1.1 Char

As for the theoretic study of this work, the unmilled straw char from the fast pyrolysis step of the bioliq process was used. The char sample was taken in December 2013 from the bioliq plant. Due to fluctuation in pyrolysis parameters in the bioliq plant, the char properties are not very constant. Table 3 shows the average properties of the char used for the bio slurry.

Table 3: properties of Char

C (%)	54.3
H (%)	1.9
N (%)	0.4
Ash content (%)	35.8
Bulk Density (kg/m^3)	250
Calorific value (MJ/kg)	20.5

The straw char contains 54.3% carbon and has also a high ash content of 35.8%. The straw char has a low bulk density of 250 kg/m^3 due to the formation of agglomerates having interspaces between the individual particles, as well as intra-particle pores. The straw char contains a high porosity of 50-80%, which strongly influences the slurry preparation because initially the liquid is drawn by capillary forces in the pores or interspaces of agglomerates, and so a significant part of the liquid is immobilized.

3.1.2 Aqueous condensate

The aqueous condensate from the bioliq plant was used for the preparation of the bio slurry. The pyrolysis condensates are less stable and have a tendency to separate in two phases. In the bioliq plant the pyrolysis vapours are condensed in two steps for obtaining an aqueous condensate and an organic condensate. The organic condensate has a high heating value of about 20 MJ/kg, so it is used directly in the gasification process. For the aqueous condensate, the heating value is about 4-7 MJ/kg, which is too low for the direct gasification. By mixing the aqueous condensate with the char the higher heating value of the mixture increase and be suitable for the gasification and.

Table 4 shows some properties of the used aqueous condensates. The organic compounds in the aqueous condensates are mainly acids, leading to a pH of 2.65.

Table 4: Properties of aqueous condensate

Water content (%)	84.8
pH	2.65
Mass density (kg/m^3)	1020
HHV (MJ/kg)	4-7

3.1.3 Bio slurry

Bio slurry is a suspension of pyrolysis condensates and pyrolysis char. In this study, the bio slurry was prepared by mixing the aqueous condensate and the char in a colloidal mixer from MAT Company. In this mixer, the shear rate is high enough to completely destroy the solid char agglomerations.

For the present study, the bio slurry with three different concentrations were prepared. At first, one ton of the bio slurry mixture was prepared in the beginning and is stored in an IBC. The concentration result is discussed in section 4.1. Due to the particle settling the mixture becomes non-homogenous after an hour. So to maintain the mixture homogenous, a motor is used to stir the bio slurry continuously at around the speed of 800 to 1000 rpm. This first prepared bio slurry named as “alpha” and used for the alpha slurry experiment.

The second bio slurry with higher concentration was prepared by adding the slurry from alpha slurry experiments and the prepared slurry named as “beta”. To increase the concentration slurry separated aqueous condensate in the alpha slurry experiment was removed and remaining higher concentrated slurry was added in the remaining alpha bio slurry in the IBC and then this mixture was stirred continuously at the same speed. The third bio slurry with higher concentration was prepared by adding the higher concentrated slurry from beta slurry experiments and the prepared slurry named as “theta”.

3.2 Experimental setup

For characterizing the particle settling of bio slurry the experiments were done in a two different scales.

3.2.1 Big scale tower

In a big scale experiment, a tower with 150 cm in height, 55 cm in breadth and 55 cm in width, which has a capacity of 450 L, was used. To sample the slurry, 25 outlets were fixed at the front side of the tower as shown in Figure 11. The distances between two outlets were 6 cm. The bio slurry was filled from the top of the tower and covered with a plate to avoid evaporation. After the defined settling time as in section

3.3, slurry samples were gathered from each outlet to measure the solid concentration by filtration. By removing the front plate, the tower was emptied and cleaned, and refilled with a new slurry of a different (higher) concentration. In the results, a first outlet at the top is considered as the outlet number 1 and followed to the last outlet as outlet number 25 at the bottom as shown in Figure 11.

Figure 11: front side of tower with outlets (a tower with 150 cm, 55 cm and 55 cm in height, breadth and width respectively, and 25 outlets at a distance of 6 cm between two outlets)

3.2.2 Small scale cylinder

For the small scale experiment, cylinders with a vertical height of 20 cm were made out of 5 segments and the bottom side is closed with a cover. Each segment has a diameter of 5 cm and a height of 4 cm. At first, two segments are joined together with tape. To increase the height of the cylinder another segment is kept in top of the fixed segments and joined with the tape. Similar process followed till the desired height obtained. For the experiments, five segments were joined together with tape to make a small settling cylinder. The resulting sedimentation tower is shown in Figure 12.

Figure 12: small scale sedimentation tower (tower height of 20 cm)

3.3 Experimental strategy

For the study of the particle settling of the bio char particles in the bio slurry, the sedimentation method was used. In the sedimentation method, the bio slurry is allowed to settle in a sedimentation tower for a set period of time. The measurement of the char concentration at different levels of the tower was determined at different time intervals of 4 hours, 8 hours, 1 day, 3 days, 7 days and 14 days. To find out the influence of the char concentration in the slurry, experiments were carried out with three different concentrated slurries. The slurry names are given as “alpha”,”beta” and”theta” and the properties of these slurries are discussed in section 4.1. With the beta slurry, experiments were done to find out the influence of the height for the particle settling in the slurry mixture. For this study, one experiment was carried out with the beta slurry in big tower filled full level (150 cm) and around half level (84 cm) and also in the small scale cylinder with (20 cm).

To find out the influences of the temperature in the settling of the particles in the slurry mixture, the experiment was performed in different temperatures, i.e. room temperatures, i.e. 20 ± 2^0C (TR), 35^0C (T35) and 45^0C (T45) in a small scale tower with the beta slurry. In the big scale tower, the experiment was done only at room temperature.

3.4 Experimental procedure for measuring the solid concentration distribution

The measurement of char concentration in the sample slurry was made by separating the char particles by filtration followed by washing the ethanol and evaporation of the liquid components.

3.3.1 Big scale tower

In a big scale tower, the slurry was taken out from each outlet and measured the weight of the sample. As the char particle is porous, it soaked the condensate and formed clusters of very low volatility. Therefore

the sample slurry is diluted with ethanol and stirred for around 20-30 seconds for proper mixing before filtration. Thus porous particles and the gaps between the particles are filled with ethanol and due to the low boiling temperature of ethanol it dried easily. Then the sample is filtered as in Figure 13 to collect char particles. After the filtration, the char is dried in the oven for minimum 6 hours at around 100^0 C to evaporate all the ethanol and condensate from the char particles. At last, the solid weight of char from each outlet was measured. By this method, we distinguished the phase separation zone and a solid concentration in different time intervals.

Figure 13: filtration of sample bio slurry

3.3.2 Small scale tower

For the measurements of the small scale tower, the towers were filled with slurries and allowed to settle for the defined sedimentation interval. Then the tape was cut stepwise from top of the column down. At first, the sample tower was kept in the beaker and the tape between the first segment and second segment was cut with the knife. So that the suspension coming out from the cutting portion is collected in the beaker. Slowly the first segment with sample was drawn out from the settling tower and kept in the beaker. Sequently with the same procedure the second, third, fourth and fifth segments were drawn out and kept in the different beaker as in Figure 14. The weights of the each beaker with the slurry sample and segment were measured. Then the slurry sample was diluted with ethanol to separate the condensate from the char particles. Then the mixtures were filtered and after a while kept in the oven for the drying for minimum 6 hours at around 100^0 C to evaporate all the ethanol and condensate from the char particles. The weight of the each beaker and the segment was measured. Thus, by subtracting the weight of the beaker and segment, the weight of slurry sample was calculated for each segment. After drying, the mass of the dried char particles from each segment was measured. With these results the phase separation and the particle settling within the slurries was distinguished.

Figure 14: sample slurries from different segments

3.3.3 Influence of temperature

To find out the influences of the temperature in the settling of the particles in the slurry mixture, the experiment was performed in different temperatures, i.e. 20^0C (TR), 35^0C (T35) and 45^0C (T45) in a small scale tower with the beta slurry. The experiments at the 20^0C were carried out in the room temperature with $\pm$ 2^0C. While for the higher temperature at 35^0C and 45^0C, the settling tower was kept in the oven as in Figure 15 till the defined settling time of 4 hours, 8 hours, 1 day, 3 days, and 7 days at the constant temperature. After the defined time, the measurement of solid concentration on each segment was followed by the same process as defined in section 3.3.2,.

Figure 15: slurry in oven at constant temperature

3.3.4 Static stability test

The stability of a slurry against gravity is called static stability. A statically unstable slurry will settle down and formed a compact sediment. While with the static stable slurry, the settling rate is less and allow the slurry flow smoothly. The factors affect the slurry stability are particle size, density, solid concentration, surface properties. The static stability of the slurry is an essential element in its applicability, which decide the value of the slurry. The static stability is significant in order for handling of the slurry likely to stirring requirement or the function of additives to minimize settling.

The calculation of bio slurry stability was carried out with a equation used for the coal water slurry method [44]. A bio slurry sample was filled in a small scale tower (with 20 cm height) and measures the weight of slurry sample. Then the slurry was kept in a room temperature for 7 days. After 7 days, the slurry tower, then was turned upright for 8 minutes to let the slurry flow adequately from the tower. Afterwards, the mass of the non-flowing parts of the bio slurry was measured. The stability of bio slurry could then be calculated using the equation:

$$S_{sta} = (1 - \frac{M_N}{M_I}) \times 100 \qquad \text{Equation 21}$$

with S_{sta} as the static stability (%), M_I as the initial mass of the bio slurry sample (g) and M_N as the mass of the non-flowing bioslurry (g).

3.3.5 Settling test in graduate cylinder

The settling of the char particles in aqueous suspension was studied in small batch experiments. A slurry of known concentration was filled in a graduate cylinder at room temperature as in Figure 16. The experiment was carried out with different initial settling height of 250 mm, 200 mm, and 150 mm. As the particle start to settle, the position of the interface between the settled particles and an almost particle free condensate was noted after a time interval of 30 min. The experiment was stopped when there was no change in the interface height. Then the height of the interface was plotted versus time. The settling velocity of the particles V_c in a suspension was determined by measuring the slope of the linear portion of the height against time.

Figure 16: batch settling in graduate cylinder

3.3.6 Viscosity measurement

Viscosity is a measurement of the resistance of fluid or suspension, which is being strained by the shear stress. The viscosity was measured with the rheometer in the. Rheometer is a device used to measure a liquid, slurry or suspension flows in response to applied forces. The rheometer are equipped with a various modular like plate-plate, cone and plate and coaxial cylinder measurement systems under controlled-stress or controlled-rate conditions.

The viscosity was measured with the rotational rheometer in the analytical lab of IKFT as shown in Figure 17. In this experiment the defined speed (shear rate) between 1 to 100 is applied and the dynamic viscosity was measured. The slurry sample was loaded into the concentric cylinder system which is designed to impose simple shear flow when rotated. Then the cylinder was kept in the holder of the rheometer and tight it with screw. And the spindle is fixed with the coupling just below the mounting. The mounting can slide up and down. For all measurements, helical spindle was used, due to its high accuracy of viscosity values and to avoid turbulent rheological regime. The spindle was fixed to the mounting by the coupling. The spindle was automatically detected by the encoder. This encoder is connected to computer by electrical wire signals which transform the mechanical action into electrical signals and show us in a graphical form by software which is “rheoplus”. When we analyze non-Newtonian fluid like in our case is a slurry of char and aqueous condensate, a plot of viscosity vs. spindle speed is constructed. Viscosity is plotted along the y-axis and speed (RPM) along the x-axis. The shape of the curve indicates the type and degree of flow behavior as shown in the Appendix A.

Figure 17: rotational rheometer setup

A: mounting, b: computer, c: spindle d: holder

4. Result

4.1 Analysis of slurry parameter

4.1.1 Slurry compositions

The analysis of the bio slurries was done by the analytic lab of the IKFT. It measured the concentration of the char and the water content in the bio slurry. Bioslurry alpha prepared from a colloidal mixture had a concentration of 23.4% char and 67.6% of water as shown in Table 5. As described in section 3.1.3, by adding higher char concentration slurry the new slurry “beta” was prepared with a char concentration of 26%. The final bio slurry “theta” has had a char concentration of 31.3%. The pH of all of the three slurries was 5.7.

Table 5: bio slurry analysis

S.N	char %	pH	H_2O %
alpha	23.4	5.7	67.6
beta	26	5.7	65.8
theta	31.3	5.7	65.5

4.1.2 Particle analysis

The size and shape of particles regulate the flow and compression properties. The smaller particles break up more and result in higher suspension rate than larger particles. Also from the Stoke’s equation, it's seen the particle size is directly proportional to the settling velocity, thus the larger particles are expected to settle faster than the small particles, but in the experiments, no different particle size distribution could be found of the height, which is justified with the high solid concentration and the hindered settling. . The particle size distributions (PSD) of bio slurry samples are shown in Table 6 and sum distribution and particle spectrum are illustrated in Appendix A. The particle size distribution X_{50} of all three slurries was below 30 μm. X_{95} for the alpha, beta and theta slurry is almost 84 μm, 80 μm, and 70 μm respectively. The mean sizes of the particles in the alpha, beta, and theta slurry were 40.7±0.6, 38.8±0.8, and 36.2±1.2 μm respectively. The decrease can be explained by the stirring treatment in the IBC.

Table 6: particle distribution for different slurries

sample	X_5 (μm)	X_{50} (μm)	X_{95} (μm)	Mean (μm)
alpha	6.32	28.98	83.87	40.7±0.6
beta	5.86	26.81	80.33	38.8±0.8
theta	5.68	26.10	70.74	36.2±1.2

4.1.3 Viscosity analysis

The viscosity is a significant parameter to characterize the slurries. The viscosity of the slurry is influenced by several parameters like temperature, particle size, particle concentration and the viscosity of the liquid medium. The viscosity was measured as a function of shear rate and temperature as illustrated in Figure 18 and Figure 19 respectively. Figure 18 describes that the characteristics of the slurries at 20^0C generally present non-Newtonian behaviour. The viscosity of the slurry varied as the shear rate was changed. Pseudo-plastic or shear thinning behaviour is characterized by the decrease in viscosity as the shear rate increases. A similar trend was found at higher temperature (i.e. 35^0C and 50^0C). The data for viscosity analysis are presented in Appendix A. It should be mentioned that the viscosity strongly decreases with increasing shear speed. Higher shear rates likely letting out the interactions and the closeness of particles thereby reducing viscosity. In this case, values with the analytically lowest possible shear speed of 1 rpm can be measure with the rotary rheometer.

As expected viscosity increases with the increase in particle concentration. Theta slurry with 31% concentration had a higher viscosity than the alpha and beta slurries with concentrations of 23% and 26% respectively. The viscosity increases because of the frictional forces between the particles become significant, and also the blockage of free condensate occur. Thus, the lubrication effect of free-flowing condensates are become ineffective [45].

Figure 19 shows the viscosity as a function of the temperature for different slurries at 50 rpm. As expected the viscosity of the slurry decreased as the temperature increased. This is because of cohesive forces between the particles decrease with the increasing temperature. Thus, the forces of attraction between particles decreases, which reduces the viscosity of the slurry. The viscosity at different shear rates are presented in Appendix A, which shows a similar trend as in Figure 19.

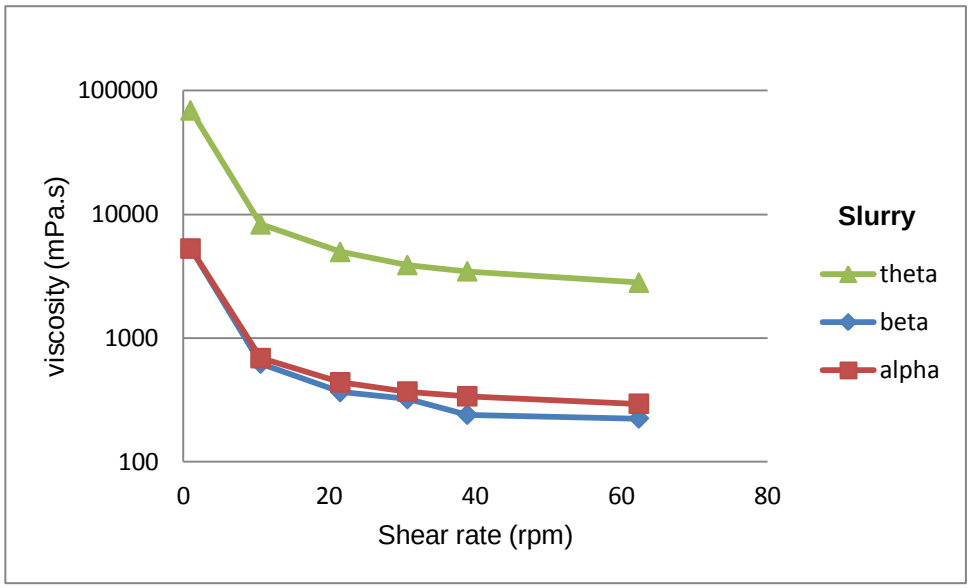

Figure 18: viscosity of slurry as a function of the shear rate at 20^0C
(theta:31.3%, beta: 26%, alpha:23.4%)

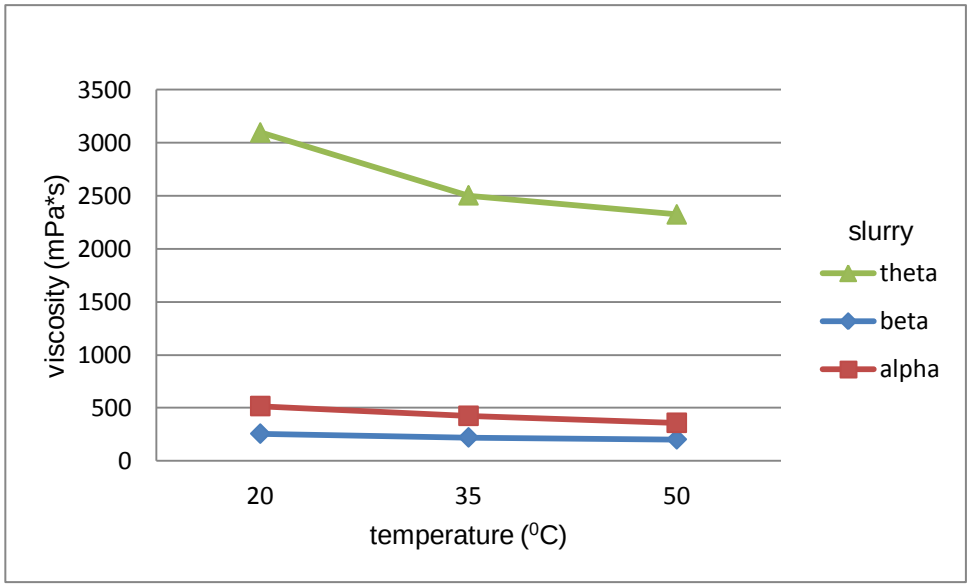

Figure 19: viscosity as the function of temperature
(theta:31.3%, beta: 26%, alpha:23.4%)

4.2 Characterization of sedimentation

In this section, the sedimentation of the bio slurry is characterized according to the influence of the char concentration, of the height of the column and of the temperature. The complete figure of all experiments is shown in Appendix B.

4.2.1 Influence of concentration of char

As mentioned in section 3.2, the experiments were done with three different concentrations with slurries named “alpha”, “beta” and “theta” and the corresponding properties were presented above in section 4.1.

Figure 20 shows the char concentration at different column levels (outlet) at different times in the experiment with slurry containing 23.4% of char. This experiment was carried out at full tower (i.e. height of 150 cm). After 24 hours, the phase separations are clearly shown in Figure 20 at the outlet number 6 (i.e. height of about 30 cm from top). In the top 5 outlets, the char concentration fell below 5%, whereas from the outlet number 7 to the outlet number 25 the char concentration increased to a maximum of 27%. In between outlet number 5 and 6, the particles fell slowly and after 336 hours the concentration on this level became nearly zero. After 72 hours, the concentration in the outlet number 7 tends to decrease steeply. Whereas, from the outlet number 8 to the outlet number 25, the slurry concentration remains nearly same till 336 hours. The maximum concentration goes to 29% on outlet number 25 on day 14.

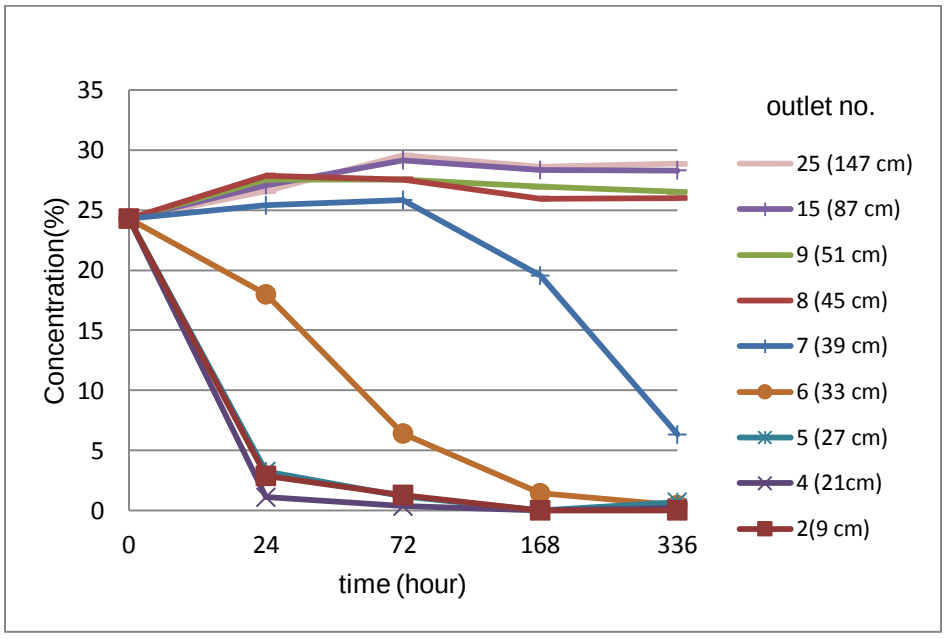

Figure 20: concentration measurement at different time intervals for alpha slurry

Figure 21 shows the char concentration at a different level in the tower at different time intervals for the “beta” slurry. In the beginning, the char concentration in the slurry was 26%. For this experiment, the

tower was filled almost half (84 cm) of the filling level of the previous experiment. The influence of the initial suspension height is presented in section 4.2.2. From outlet number 16 to outlet number 25 the concentration rises up to 31% from the initial concentration after 4 hours and then increased very slowly to a maximum of around 33% till 336 hours. Whereas in first two outlets (i.e. height of about 9 cm) the concentration went down below 5% in 4 hours and tended to zero percent concentration after 8 hours. After 24 hours, it was possible to obtain an almost clear aqueous phase in the first three outlets (from outlet number 12 to 14 i.e. height of about 15 cm). After 24 hours, particles settle slowly in between outlet number 15 and 16 (height of 21 cm to 27 cm). At 336 hours, outlet number 15 became a nearly char free zone, while the concentration at outlet number 16 goes down to 7%.

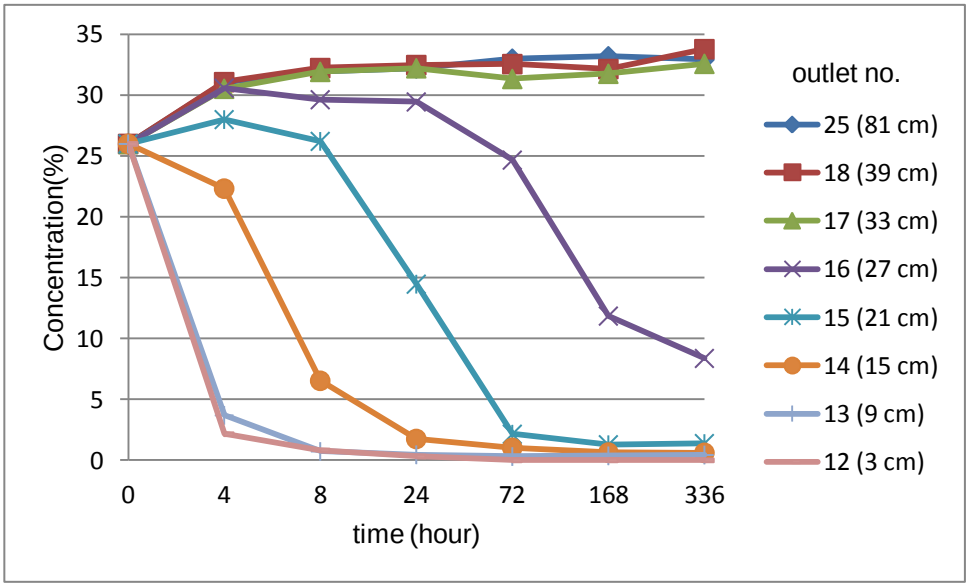

Figure 21: concentration measurement at different time intervals for beta slurry

Figure 22 shows the results for the “theta” slurry with a concentration of 31.4%. As for the experiment with the beta slurry, this experiment was also carried out with the tower half filled. Thus, after 24 hours, almost all char particles settled down below the height of 15 cm correspondent to the outlet 14. On the bottom of the tower i.e.outlet 25, the char concentration is almost same to the initial concentration. After 72 hours, there was no significant change in the char concentration in any level of the tank. The maximum concentration goes to 34% in outlet number 25 after 336 hours.

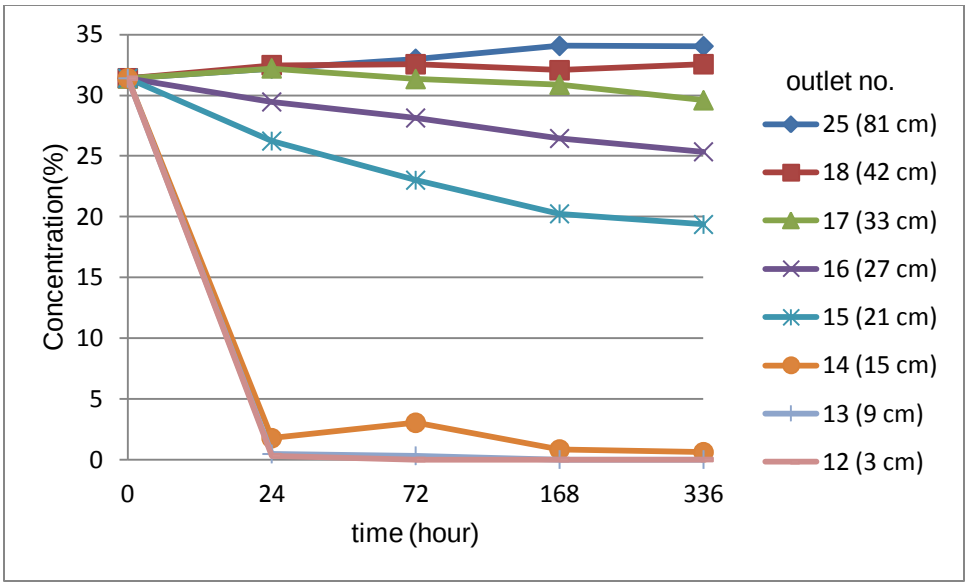

Figure 22: concentration measurement at different time interval for theta slurry

Comparing the results obtained with slurry theta and beta it can be seen that with the higher concentration of the slurry the lesser the concentration change at the lower level corresponding to the outlet number 25. In fact, it seems likely that the initial concentration of around 31% is closer to the maximum packing density. Also, it can be seen that after 24 hours a relative sediment concentration has formed from outlet number 8 for alpha slurry and outlet number 17 for beta slurry and from outlet number 15 for the theta slurry. After this, the particle settling process becomes slower because the displaced liquid has to flow through the small spaces between the particles and the resistance to the flow of liquid progressively increases.

From the above figures, it is also possible to conclude that that the rate of settling of the particles tends to decrease as the concentration of particles approaches a limiting value corresponding to that of the sediment layer deposited at the bottom of the tower. With higher concentrations of particles in the suspension, interactions between the particles increase and limit the movement of the particle relative to each other.

Comparing the results presented in Figure 21 and Figure 22, it is possible to conclude that the concentration changes after 24h were lower in the experiment with the theta slurry. In fact, for this slurry the larger variation obtained was off about 5% in the outlets 15, whereas for the beta slurry, the decrease of the concentration was off about 15% in the same outlets. At 336 hours, it was observed that, slurry with an initial concentration of 31.3% (theta slurry), the interface level between the particles and condensate is up to the height of 15 cm. Whereas, slurry with a lower concentration of about 26% (beta slurry), particles tend to settle down around the height of up to 21 cm.

With the Equation 19, the average concentration of the sediments may be calculated from the data in Table 7 obtained from the experiments. The average concentration was initial concentration times the initial height by sediment height. The result of average concentration of the sediment was calculated as in Table 7. This shows that the calculated average concentration is nearly the same concentration obtained from the experiment.

Table 7: average concentration of sediment

Initial slurry concentration (%)	Initial height (cm)	Interface height (cm)	Relative interface level (%)	Sediment height (cm)	Average concentration of sediment (%)
23.4	150	33	22	117	30
26	84	21	25	63	34.7
31.3	84	15	17.9	69	38.01

4.2.2 Influence of settling height

For the study of the influence of the height as described in section 3.3, the big tower was filled full level (150 cm) and around half level (84 cm) with a beta slurry (26% char content) and experiment was also carried out in the small scale cylinder (20 cm) with the beta slurry.

Figure 23 shows the settling of char particles as a function of the relative height at different time intervals. After 8 hours, phase separation was seen at the relative height of 30% in all three initial heights. In relative height higher than 30% the concentration of the char is increased to maximum packing density. After 1 day, there was no significant change in the char concentration in all experiments from 40 % relative heights to end of the tank. After day 3, in the top level, i.e. to 20% relative heights, the char concentration was almost zero in all three experiments and at the lower level there is no significant change in the char concentration. After 7 days, the interface level is almost to 20% relative height in all experiments.

The result clearly shows that, the height of the settling tower did not affect either the settling trend or the consistence of the sedimentation. From all these figures at different interval of time, there the concentration of the char particles in different level or relative height is almost same and the solid concentration in the bottom region was also almost the same. This means that the hydrostatic pressure of the suspension did not influence the particle settling. Therefore, small scaled experiments can be scaled up.

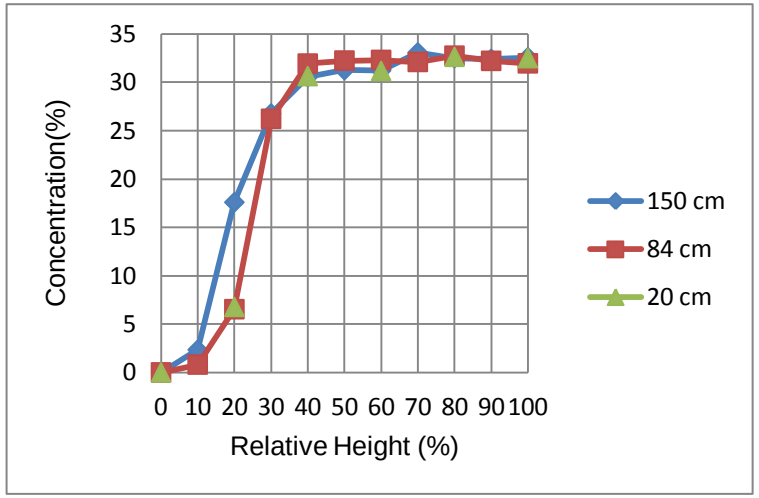

(a)

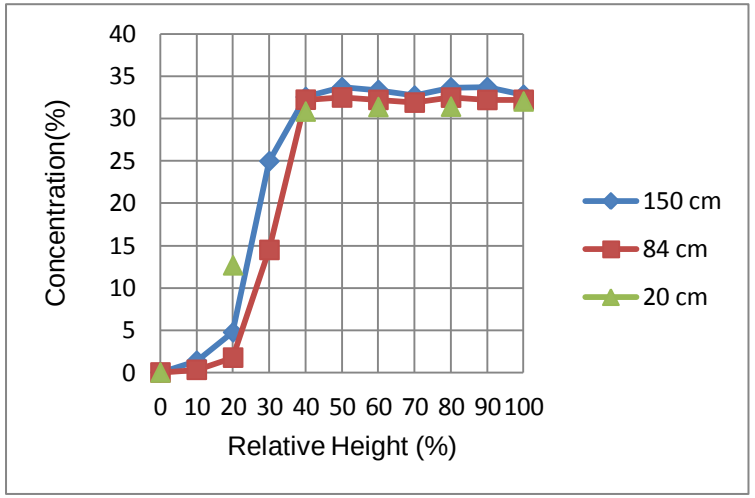

(b)

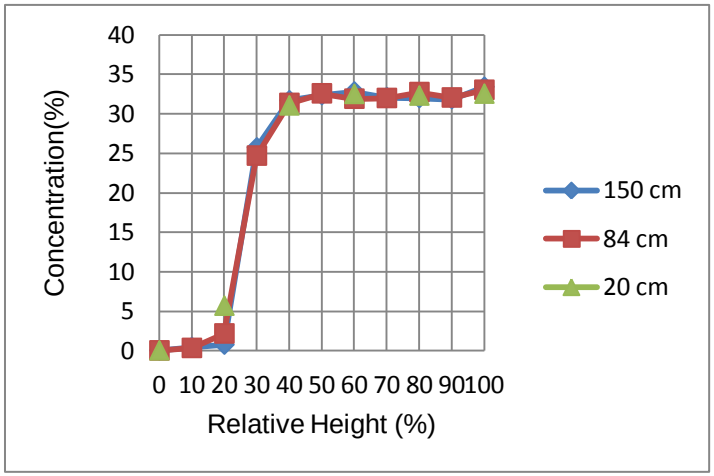

(c)

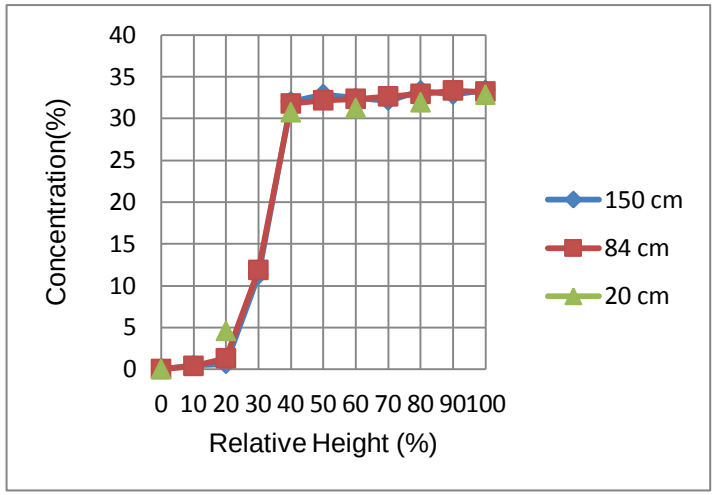

(d)

Figure 23: char concentration as a function of the column height (a) after 8 hours, (b) after 1 day, (c) after 3 days, (d) after 7 days

4.2.3 Influence of temperature

Figure 24 and Figure 25 show the influence of the temperature and time and the sedimentation of char for the beta slurry. The result shows that the settling of the char at room temperature (20±2^{0}C) is lower than at a temperature of 35^{0}C and 45^{0}C. From Figure 24 (b), (c), (d) and (e) it can be seen that the concentration at a temperature of 35^{0}C and 45^{0}C fell slowly in top segments and slightly increased in the bottom segments. At room temperature the concentration from the second segment to last segment seemed constant after 4 hours.

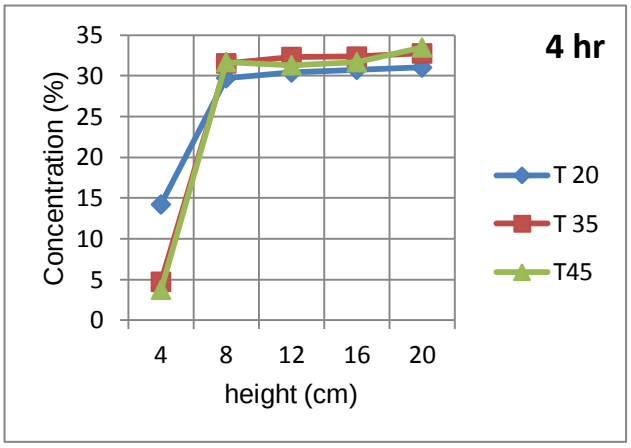

(a)

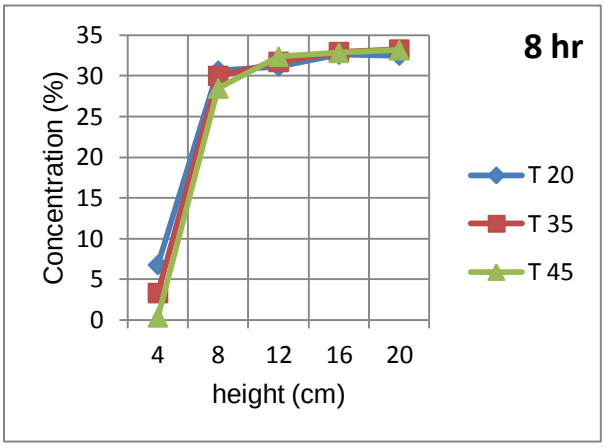

(b)

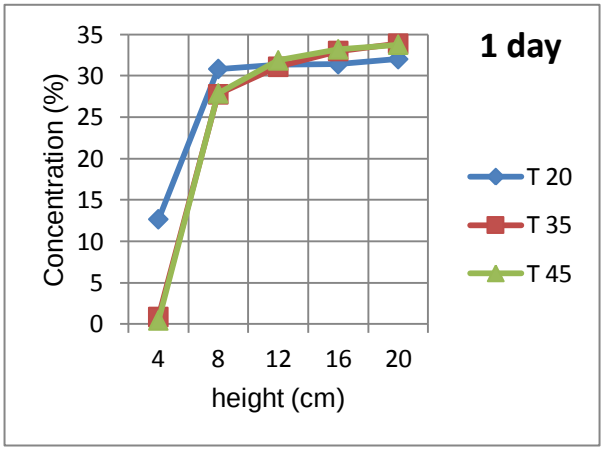

(c)

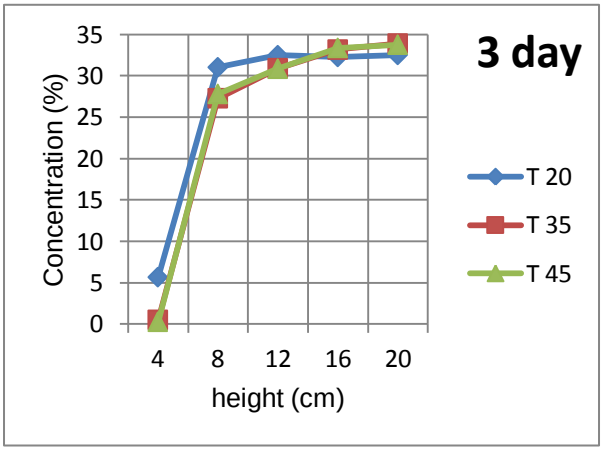

(d)

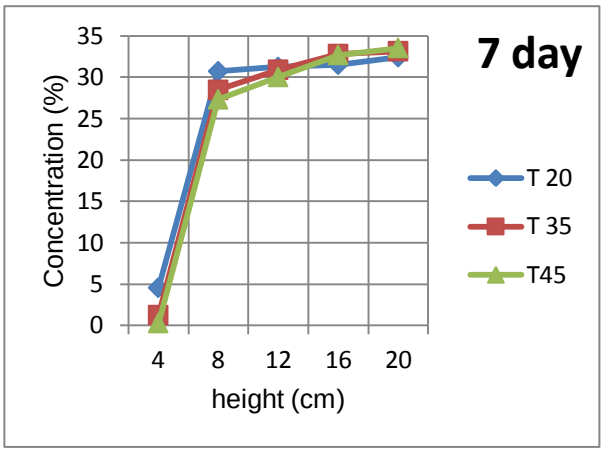

(e)

Figure 24: concentration of char as a function of temperature (a) after 4 hours, (b) after 8 hours, (c) after 1 day, (d) after 3 days, (e) after 7 days

Figure 25 shows the previous results, but only for the first segment (height 4 cm) and the last segment (height 20 cm). Thus, it is clear that the increase of the temperature favours the sedimentation rate because after 4 hours, at room temperature (20±2^{0}C) the concentration of char at the top segments goes down to 14%, while at 35^{0}C and 45^{0}C this concentration is 5% and 4% respectively. In the bottom segments, the char concentration at room temperature (20±2^{0}C) and at a temperature 35^{0}C and 45^{0}C has a difference of around 3%. However, for the bottom segment the influence of the temperature is not important. These results indicate that, in order to avoid the sedimentation of the char particles, it is better to store the bioslurry at lower temperature.

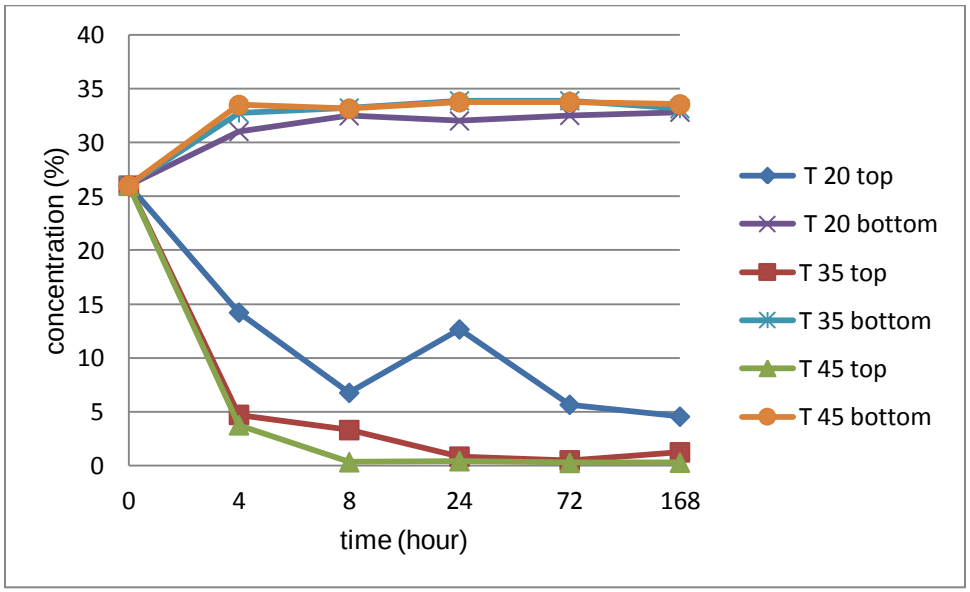

Figure 25: concentration as a function of temperature for first (top) segment and last (bottom) segment

4.3 Static stability

To estimate the bio slurry stability, the standard method for coal water slurry was adapted. For the coal water slurry (CWS), a stability of more than 70% was suggested [23][23] . As illustrated in Figure 26, using the same method, the static stability for the beta slurry and theta slurry was found at 80 % and 79% respectively. Liu et al.[44] refer a stability of 90% for a CWS with a concentration of 62.7 % and Abdulla [23] present a stability of 82% for 20% concentration of biochar in biooil of malle biomass.

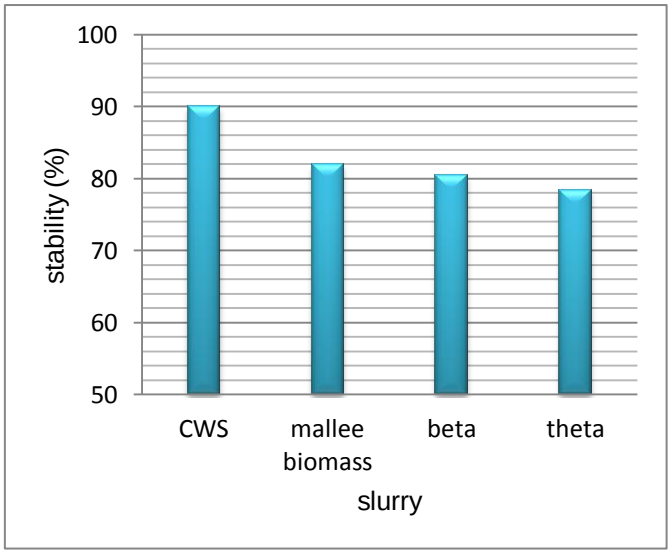

Figure 26: static stability of bioslurry

4.4 Settling test in a graduate cylinder

The settling behaviour of slurries in a batch settling test is illustrated in Figure 27, which shows the settling rate of alpha, beta and theta slurry samples in a sedimentation cylinder as a function of time for different initial settling heights of 250 mm, 200 mm, and 150 mm. The figures show the same trend. At the beginning of the experiment, the concentration is uniform throughout the cylinder. After a short time, a sharp interface is formed, separating the clear liquid in the upper part and settling particles in the lower part. For a period of time particles settles at a uniform rate. By the time in the lower section of the cylinder, particles with a higher concentration amass. After a while, the particle-liquid interface approaches the region of concentrated particles and its rate of displacement starts to fall gradually because the resistance to the upwards flow of condensate through the particle increases. Also the porosity of the sediment has been found less at the lower section because of the self-weight of particles [46]. After some time, the settling rate becomes almost constant over the increasing time.

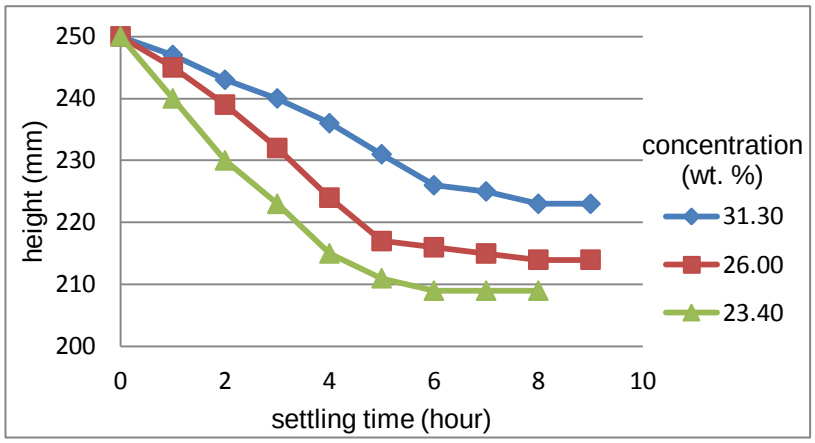

(a)

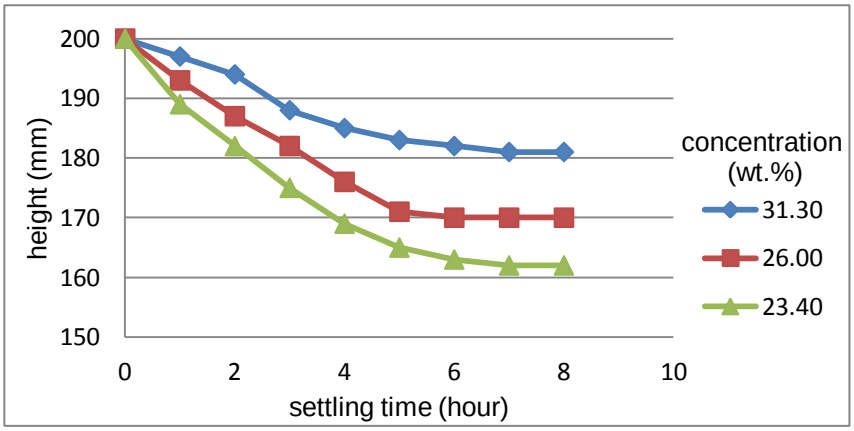

(b)

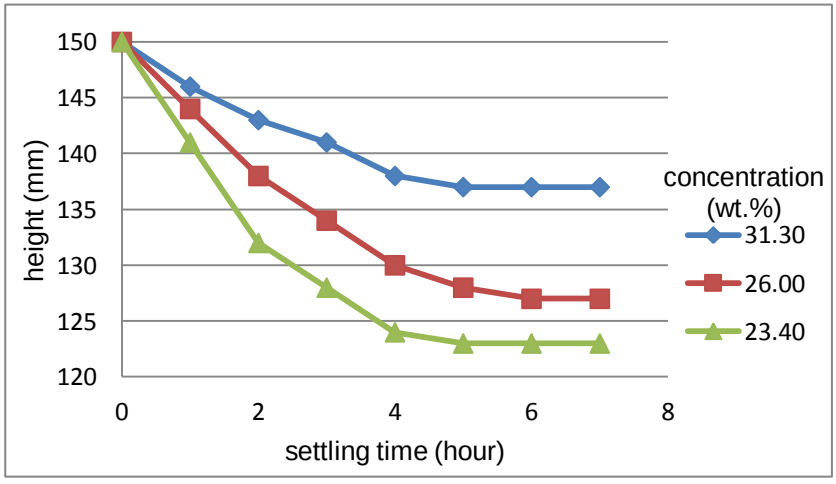

(c)

Figure 27: interface height against time plots for zone settling of different concentration slurries (a) at the initial settling height of 250 mm, (b) at the initial settling height of 200 mm (c) at the initial settling height of 150 mm

From the slope of the linear decreasing portion of the settling curve, zone settling velocity of the particles V_c in aqueous condensate suspension was determined and the results are presented in Table 8. The measured values show that, the settling velocity decrease with increasing concentration. A similar trend was found in the big scale experiment as discussed in section 4.2.1. Furthermore, with the standard deviations , it is possible to conclude that the height has no influence.

Table 8: settling velocity of suspension for alpha slurry (23.4%), beta slurry (26%) and theta slurry (31.3%)

	settling velocity (mm/h) / concentration (wt. %)		
height (mm)	23.4	26	31.3
250	7.9±2.2	6.7±1.1	4±0.9
200	6.9±2.2	5.7±0.6	3.6±0.4
150	6.5±1.7	5±1.0	3±0.6

5. Conclusion and Recommendation

5.1 Conclusion

In this study, unmilled pyrolysis char and the aqueous condensate from the bioliq plant were used to prepare bio slurries. The research of these suspensions was done to check the influence of the char concentration in the suspension, of the settling height of the tower and of the temperature on the char particles settling

Three bio slurries identified as “alpha”, “beta”, and “theta” with respectively, 23.4 wt. %, 26 wt. %, and 31.3 wt. % of char particles were used in this work. The particle size distribution of all three of the slurries corresponds to an X_{50} was below 30 μm and X_{95} was below 85 μm. From the viscosity analysis, the bioslurries characteristic showed non-Newtonian behaviour and pseudo-plastic or shear thinning behaviour because their viscosity decreases as the shear rate increases. Furthermore, the viscosity of the slurry increase with the increase of the particle concentration, but as expected decreases with increasing the temperature.

It observed that, the interface level between the aqueous condensate and the char particles is lower for the higher char concentration suspension than at the lower char concentration suspension. The settling rate was lower for the most concentrated slurry because the resistance to the upward flow of the fluid increases. This is also the reason why the settling in the bottom side of the tower was the slowest part of the process because the displaced fluid had to flow through the small spaces between the particles. Also, it seemed that with a higher initial concentration of 31.3% the particle moved closer to the maximum packing density, thus there were fewer changes in the concentration at the lower levels.

It was also found that the sedimentation rate of the char particles and the solid concentration in the bottom region are not affected by the change of initial settling height. Thus, it can be concluded that the hydrostatic pressure of the suspension has no impact on the particles settling. Therefore, small scaled experiments can be scaled up.

As an increasing the storage temperature from room temperature to a temperature of 35^0C and 45^0C, the increase in the settling rate. Therefore, it is possible to conclude that for storing the bioslurry lower temperatures are better suited.

Finally, using the Kynch theory of sedimentation, the settling velocity of the particles in the suspension was calculated. The settling velocity of the particles decreased with the increased of the suspension concentration and height has no influence.

The phase separation occurs within an hour, so it is recommended to keep the slurry stable and homogeneous by a continuous stirring process.

5.2 Future Work

In this study, unmilled pyrolysis bio char was used to prepare the bioslurry. Further studies can be carried out with the milled bio char. By milling the bio char, the particle size distribution of the char particle is approximately divided in half. With smaller particle sizes, higher solid concentrations can be achieved, which also lead to more viscous slurry, and therefore to decreased settling rates.

The char from pyrolysed wheat straw has a high content of ash at around 30-40%. This ash may contain different minerals that can contribute to increasing settling rates of the char particles in the suspension. Thus, the effect of the ash contents on the sedimentation rate needs to be researched.

Furthermore, the study of the use of additives to maintain the stability of the suspension of bio char in the aqueous condensate is also important.

6. Bibliography

[1] "International Energy Agency: World Energy Outlook."

[2] Energy Information Administration(EIA), "No Title," 2008. [Online]. Available: http://tonto.eia.doe.gov/energyexplained/index.cfm.

[3] R. W. R. Zwart and H. Boerrigter, "High efficiency co-production of synthetic natural gas (SNG) and Fisher–Tropsh (FT) transportation fuels from biomass," *Energy Fuels*, vol. 19, pp. 591–597, 2005.

[4] A. Demirbas, "Competitive liquid biofuels from biomass," *Appl. Energy*, vol. 88, no. 2011, pp. 17–28.

[5] E. Sadeghinezhad, S. N. Kazi, F. Sadeghinejad, A. Badarudin, M. Mehrali, R. Sadri, and M. R. Safaei, "A comprehensive literature review of bio-fuel performance in internal combustion engine and relevant costs involvement," *Renew. Sustain. Energy Rev.*, vol. 30, no. 2014, pp. 29–44.

[6] A. Sultana and A. Kumar, "Development of tortuosity factor for assessment of lignocellulosic biomass delivery cost to a biorefinery," *Appl. Energy*, vol. 119, pp. 288–295, Apr. 2014.

[7] E. Henrich, N. Dahmen, and E. Dinjus, "Cost estimate for biosynfuel production via biosyncrude gasification," *Biofuels, Bioprod. Biorefining*, vol. 3, no. 1, pp. 28–41, Jan. 2009.

[8] N. Dahmen, E. Dinjus, and E. Henrich, "from the Biomass," pp. 61–65, 2008.

[9] N. Dahmen, E. Dinjus, and E. Henrich, "Synthesis gas from biomass - Problems and solutions en route to technical realization," *Oil Gas-European Mag.*, vol. 33, no. 1, pp. 31–34, 2007.

[10] N. Dahmen, E. Henrich, E. Dinjus, and F. Weirich, "The bioliq® bioslurry gasification process for the production of biosynfuels, organic chemicals, and energy," *Energy. Sustain. Soc.*, vol. 2, no. 1, p. 3, 2012.

[11] C. Kornmayer, E. Dinjus, E. Henrich, and F. Weirich, "Advanced Fast Pyrolysis of Lignocellulose in a Twin Screw Mixer Reactor," *DGMK-Fachbereichstagung „Energetische Nutzung von Biomassen*, no. April, p. 2006, 2006.

[12] E. Henrich, "The status of the FZK concept of biomass gasification," *Summer Sch. Univ. Warsaw*, no. August, pp. 29–31, 2007.

[13] "Biomass potential - Agriculture and rural development." [Online]. Available: http://ec.europa.eu/agriculture/bioenergy/potential/index_en.htm. [Accessed: 23-Sep-2014].

[14] H. Jørgensen, "Enzymatic conversion of lignocellulose into fermentable sugars: challenges and opportunities," *Biofuels, Bioprod. …*, pp. 119–134, 2007.

[15] P. Harmsen, W. Huijgen, L. Bermudez, and R. Bakker, *Literature review of physical and chemical pretreatment processes for lignocellulosic biomass*, no. September. 2010, pp. 1–49.

[16] F. Shafizadeh, "Introduction to pyrolysis of biomass," *Anal. Appl. Pyrolysis*, vol. 3, pp. 283–305, 1982.

[17] S. D. Stefanidis, K. G. Kalogiannis, E. F. Iliopoulou, C. M. Michailof, P. a. Pilavachi, and A. a. Lappas, “A study of lignocellulosic biomass pyrolysis via the pyrolysis of cellulose, hemicellulose and lignin,” *J. Anal. Appl. Pyrolysis*, vol. 105, pp. 143–150, Jan. 2014.

[18] S. Sinha, A. Jhalani, M. Ravi, and A. Ray, “Modelling of pyrolysis in wood: A review,” *SESI J.*, pp. 1–17, 2000.

[19] N. Tröger, D. Richter, and R. Stahl, “Effect of feedstock composition on product yields and energy recovery rates of fast pyrolysis products from different straw types,” *J. Anal. Appl. Pyrolysis*, vol. 100, pp. 158–165, Mar. 2013.

[20] V. Kalpesh and D. Shyam, “Review of charcoal-Diesel slurry: An Alternative fuel for compression Ignition Engine,” *Int. J. …*, vol. I, 2012.

[21] F. Ohen, K. Bowman, A. Williams, and B. Obonna, “Temperature and high shear viscosity on the handling of coal-water slurries.”

[22] H. Wu, Y. Yu, and K. Yip, “Bioslurry as a Fuel . 1 . Viability of a Bioslurry-Based Bioenergy Supply Chain for Mallee Biomass in Western Australia,” no. 12, pp. 5652–5659, 2010.

[23] H. Abdullah, D. Mourant, C.-Z. Li, and H. Wu, “Bioslurry as a Fuel 3. Fuel and Rheological properties of Bioslurry prepared from the Bio-oil and Biochar of mallee Biomass Fast Pyrolysis,” *Energy Fuelsnergy Fuels*, 2010.

[24] V. P. Natarajan, “Rheological studies on a slurry biofuel to aid in evaluating its suitability as a fuel,” vol. 76, no. 14115, pp. 1527–1535, 1997.

[25] M. M. Benter, I. A. Gilmourt, and L. Arnoux, “Biomass-oil slurry fuels: An Investigation into their preparation and formulation,” *Biomass and Bioenergy*, vol. 12, no. 1997, p. 253 261.

[26] W. He, C. S. Park, and J. M. Norbeck, “Rheological Study of Comingled Biomass and Coal Slurries with Hydrothermal Pretreatment,” *Energy Fuels*, vol. 23, no. 2009, pp. 4763–4767, 2009.

[27] M.-K. H. Winkler, J. P. Bassin, R. Kleerebezem, R. G. J. M. van der Lans, and M. C. M. van Loosdrecht, “Temperature and salt effects on settling velocity in granular sludge technology,” *Water Res.*, vol. 46, no. 16, pp. 5445–5451, Oct. 2012.

[28] K. E. Ugwu, “Influence of Solid Concentration on the Flow Characteristics and Settling Rate of Coal-Water Slurries,” *J. Energy Nat. Resour.*, vol. 2, no. 3, p. 21, 2013.

[29] V. R. Koka, G. Papachristodoulou, and O. Trass, “Settling stability of coal sluries prepared by wet grinding in the szego mill.”

[30] C. T. Friedrichs and S. J. Smith, “Size and settling velocities of cohesive flocs and suspended sediment aggregates in a trailing suction hopper dredge plume.”

[31] Holdich Richard G, *Fundamentals of Particle Technology*. Midland Information and Technologyand publishing.

[32] J. F. Richardson and W. N. Zaki, “Sedimentation and fluidisation: Part I,” *Chem. Eng. Res. Des.*, vol. 75, no. 3, pp. S82–S100, Dec. 1997.

[33] F. Concha and E. Almendra, “Settling velocities of particulate systems, 2. Settling velocities of suspensions of spherical particles,” *Int. J. Miner. Process.*, vol. 6, pp. 31–41, 1979.

[34] B. Renzo, D. Felice, and R. Kehlenbeck, “Sedimentation Velocity of Solids in Finite Size Vessels,” vol. 23, pp. 1123–1126, 2000.

[35] G. B. Wallis, *One Dimensional Two Phase Flow*. McGraw-Hill, 1969.

[36] B. Claus, *Particle size Analysis Classificarion and Sedimentation Method*, First edit. Chapman ande hall, 1994.

[37] T. Allen, *Particle Size Measurement*, Fourth Edi. Chapman and Hall, 1990.

[38] P. Li, D. Yang, H. Lou, and X. Qiu, “Study on the stability of coal water slurry using dispersion-stability analyzer,” *J. Fuel Chem. Technol.*, vol. 36, no. 5, pp. 524–529, Oct. 2008.

[39] B. Y. G. J. Kynch, “A theory of sedimentation,” 1951.

[40] L. Cui, L. An, and H. Jiang, “A novel process for preparation of an ultra-clean superfine coal–oil slurry,” *Fuel*, vol. 87, no. 10–11, pp. 2296–2303, Aug. 2008.

[41] W. Li, W. Li, and H. Liu, “The resource utilization of algae—Preparing coal slurry with algae,” *Fuel*, vol. 89, no. 5, pp. 965–970, May 2010.

[42] M. Liu, Y. Duan, and H. Li, “Effect of modified sludge on the rheological properties and co-slurry mechanism of petroleum coke–sludge slurry,” *Powder Technol.*, vol. 243, pp. 18–26, Jul. 2013.

[43] P. Shivaram, Y. K. Leong, H. Yang, and D. K. Zhang, “Flow and yield stress behaviour of ultrafine Mallee biochar slurry fuels: The effect of particle size distribution and additives,” *Fuel*, vol. 104, pp. 326–332, Feb. 2013.

[44] J. Liu, W. Zhao, J. Zhou, J. Cheng, G. Zhang, Y. Feng, and K. Cen, “An investigation on the rheological and sulfur-retention characteristics of desulfurizing coal water slurry with calcium-based additives,” *Fuel Process. Technol.*, vol. 90, no. 1, pp. 91–98, Jan. 2009.

[45] S. K. Mishra, P. K. Senapati, and D. Panda, “Rheological Behavior of Coal-Water Slurry,” *Energy Sources*, vol. 24, no. 2, pp. 159–167, Feb. 2002.

[46] C. J. M and R. J. F, *Chemical Engineering, Vol. II Particle Technology and Seperation process*, Fourth Edi. Pergamon Press, New York, 1991.

7. Appendix

7.1 Appendix A: Lab results of bioslurry analysis

Particle size distribution

Table 9: PSD statistics for alpha slurry measurement 1

Mean	40.2855	Std	24,2189	Number	1788558.0000
X (1,0)	9.2134	X (3,2)	26.5732	X (4,3)	40.2855
X (5%)	6.3561	X (50%)	29.3611	X (95%)	82.1665

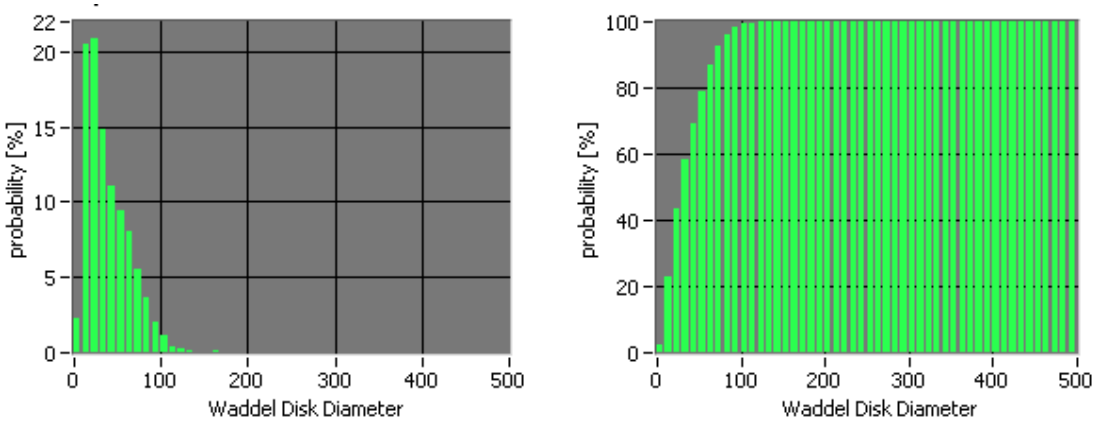

(a) (b)

Figure A. 1: PSD for alpha slurry measurement 1 (a) particle spectrum, (b) sum distribution

Table 10: PSD statistics for alpha slurry measurement 2

Mean	41.1114	Std	24.9793	Number	2230514
X (1,0)	9.2268	X (3,2)	26.9430	X (4,3)	41.1114
X (5%)	6.4243	X (50%)	29.8764	X (95%)	84.9230

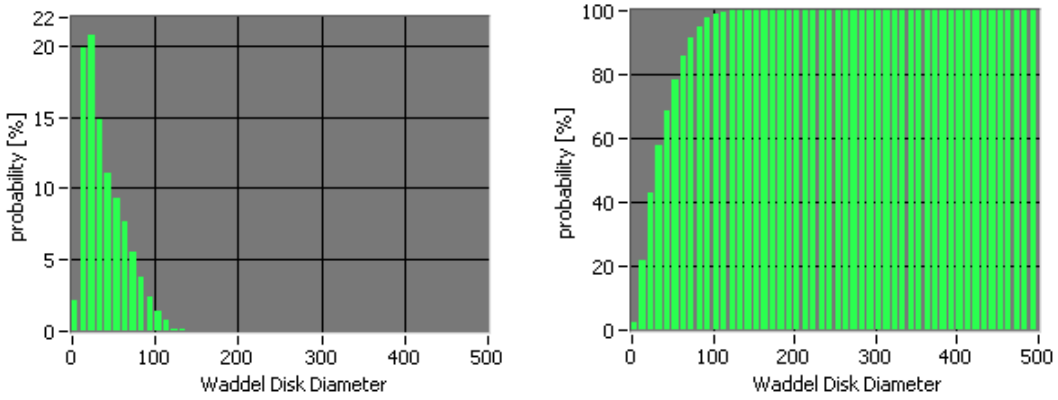

(a) (b)

Figure A. 2: PSD for alpha slurry measurement 2 (a) particle spectrum, (b) sum distribution

Table 11: PSD statistics for beta slurry measurement 1

Mean	39.1374	Std	24.6458	Number	1949572
X (1,0)	8.6306	X (3,2)	24.9040	X (4,3)	39.1374
X (5%)	5.8861	X (50%)	27.1417	X (95%)	81.6455

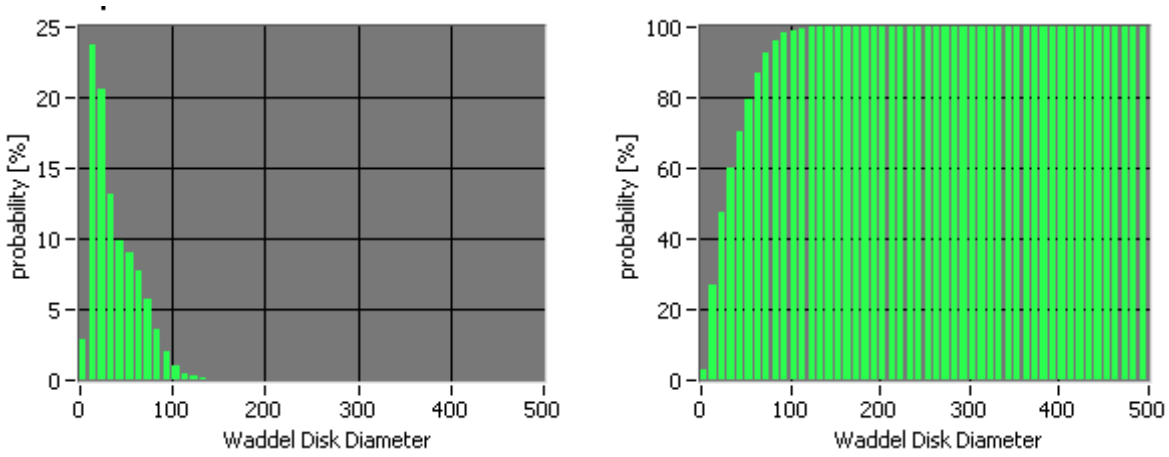

(a) (b)

Figure A. 3: PSD for beta slurry measurement 1 (a) particle spectrum, (b) sum distribution

Table 12: PSD statistics for beta slurry measurement 2

Mean	38.0566	Std	23.5649	Number	1760988
X (1,0)	8.6346	X (3,2)	24.5370	X (4,3)	38.0566
X (5%)	5.8429	X (50%)	26.4824	X (95%)	79.0305

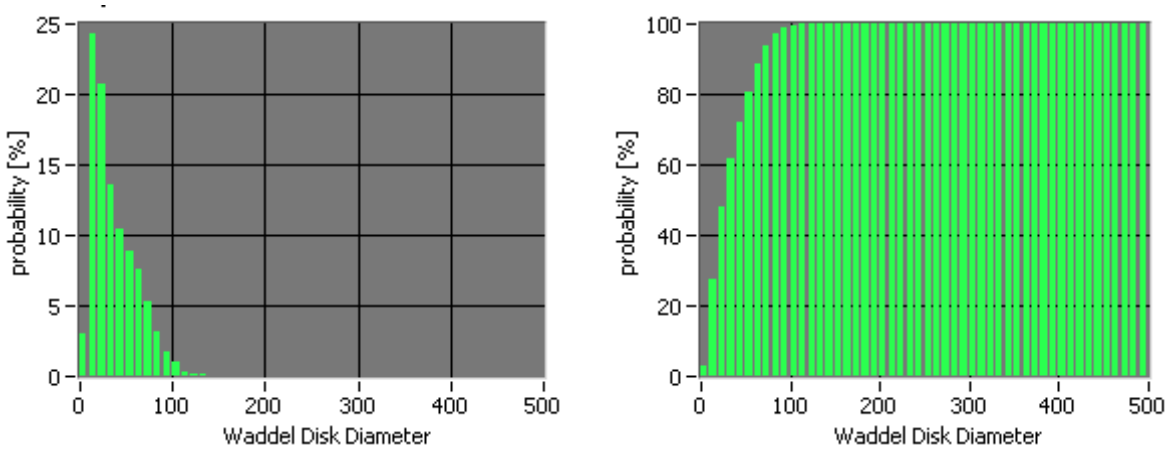

(a) (b)

Figure A. 4: PSD for beta slurry measurement 2 (a) particle spectrum, (b) sum distribution

Table 13: PSD statistics for theta slurry measurement 1

Mean	35.3500	Std	20,5474	Number	820362
X (1,0)	8.3717	X (3,2)	23,3838	X (4,3)	35.3500
X (5%)	5.6134	X (50%)	25,1301	X (95%)	69.5908

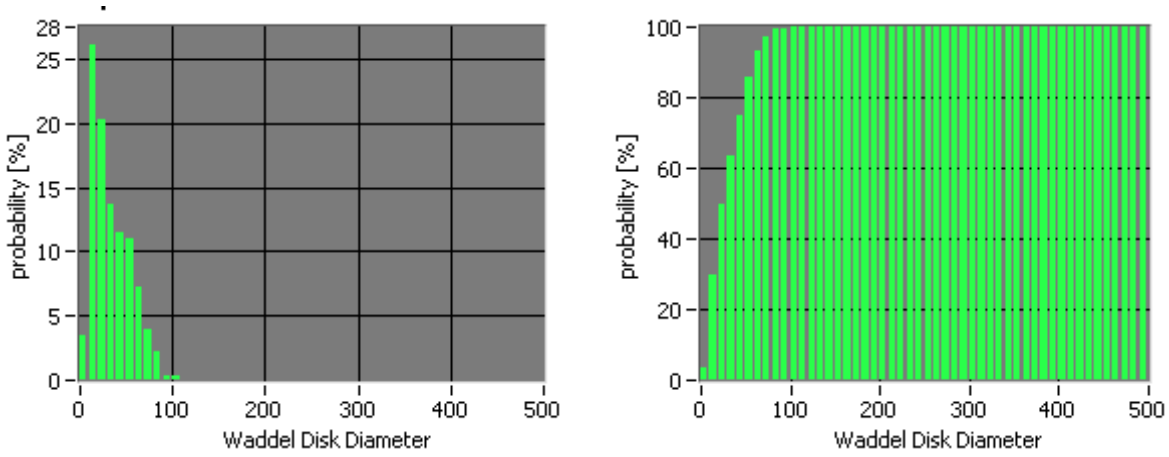

(a) (b)

Figure A. 5: PSD for theta slurry measurement 1 (a) particle spectrum, (b) sum distribution

Table 14: PSD statistics for theta slurry measurement 2

Mean	37.0808	Std	21,5379	Number	1248879
X (1,0)	8.4167	X (3,2)	24,2949	X (4,3)	37.0808
X (5%)	5.7469	X (50%)	27,0792	X (95%)	71.8961

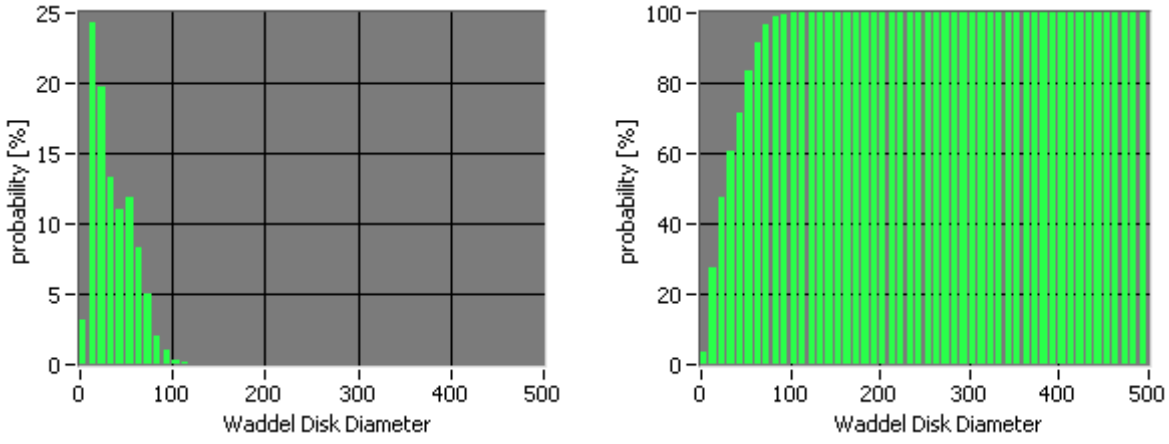

(a) (b)

Figure A. 6: PSD for theta slurry measurement 2 (a) particle spectrum, (b) sum distribution

Viscosity measurement

Table 15: viscosity measurement for alpha slurry at 20^0C

S No.	Shear rate	Viscosity	S No.	Shear rate	Viscosity	S No.	Shear rate	Viscosity
	[1/min]	[mPa·s]		[1/min]	[mPa·s]		[1/min]	[mPa·s]
1	1	5280	11	7.44	886	21	30.7	369
2	1.13	4590	12	8.38	815	22	34.6	352
3	1.27	3940	13	9.43	745	23	43.8	325
4	2.03	2590	14	10.6	687	24	49.2	316
5	3.26	1720	15	11.9	634	25	55.4	307
6	4.12	1410	16	15.1	544	26	62.4	294
7	4.64	1280	17	17	503	27	70.2	278
8	5.22	1160	18	19.1	468	28	79	258
9	5.88	1060	19	21.5	438	29	88.9	241
10	6.61	969	20	24.2	411	30	100	222

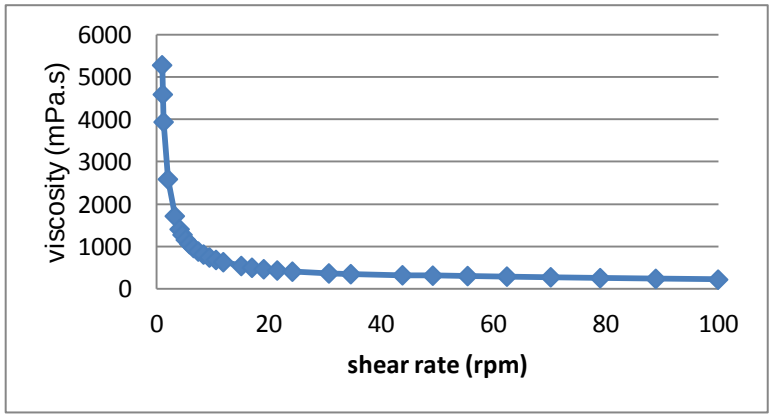

Figure A. 7: viscosity against shear rate for alpha slurry at 20^0C

Table 16: viscosity measurement for alpha slurry at 35^0C

S No.	Shear rate	Viscosity	S No.	Shear rate	Viscosity	S No.	Shear rate	Viscosity
	[1/min]	[mPa·s]		[1/min]	[mPa·s]		[1/min]	[mPa·s]
1	1	5390	11	10.6	679	21	34.6	311
2	1.13	4610	12	11.9	623	22	38.9	292
3	1.27	3980	13	13.4	572	23	43.8	275
4	2.03	2590	14	15.1	526	24	49.2	261
5	3.26	1730	15	17	486	25	55.4	249
6	4.12	1420	16	19.1	448	26	62.4	238
7	5.22	1180	17	21.5	415	27	70.2	229
8	6.61	970	18	24.2	386	28	79	219
9	8.38	812	19	27.3	358	29	88.9	213
10	9.43	739	20	30.7	333	30	100	209

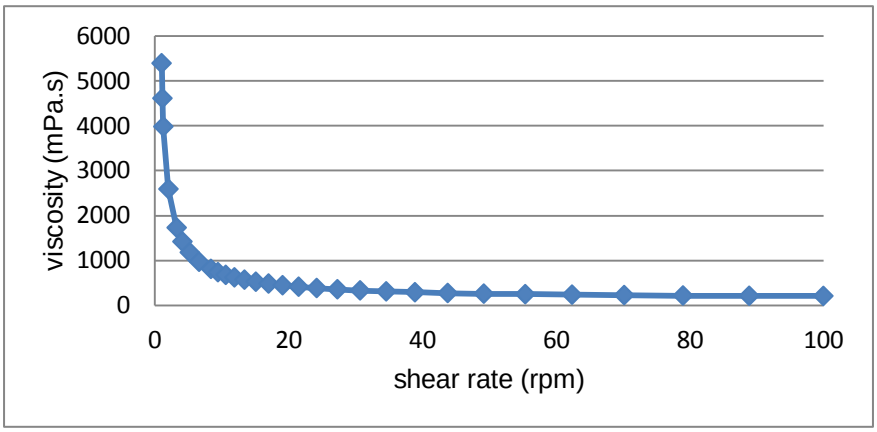

Figure A. 8: viscosity against shear rate for alpha slurry at 35^{0}C

Table 17: viscosity measurement for alpha slurry at 50^{0}C

S No.	Shear rate	Viscosity	S No.	Shear rate	Viscosity	S No.	Shear rate	Viscosity
	[1/min]	[mPa·s]		[1/min]	[mPa·s]		[1/min]	[mPa·s]
1	1	6230	11	10.6	751	21	34.6	318
2	1.13	5220	12	11.9	685	22	38.9	294
3	1.27	4550	13	13.4	624	23	43.8	273
4	2.03	2800	14	15.1	572	24	49.2	253
5	3.26	1900	15	17	523	25	55.4	235
6	4.12	1600	16	19.1	481	26	62.4	218
7	5.22	1310	17	21.5	443	27	70.2	204
8	6.61	1090	18	24.2	405	28	79	190
9	8.38	902	19	27.3	374	29	88.9	182
10	9.43	823	20	30.7	345	30	100	172

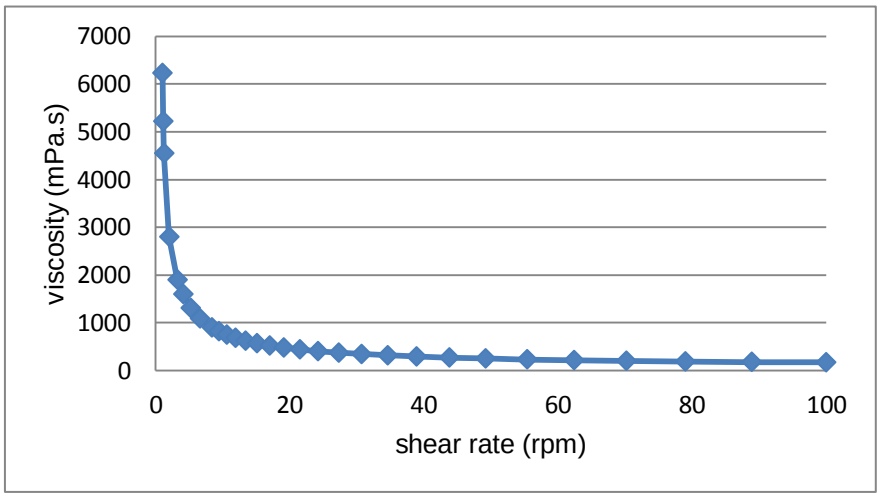

Figure A. 9: viscosity against shear rate for alpha slurry at 50^{0}C

Table 18: viscosity measurement for beta slurry at 20^0C

S No.	Shear rate	Viscosity	S No.	Shear rate	Viscosity	S No.	Shear rate	Viscosity
	[1/min]	[mPa·s]		[1/min]	[mPa·s]		[1/min]	[mPa·s]
1	1	5270	11	11.9	571	21	38.9	288
2	1.27	4050	12	13.4	525	22	43.8	271
3	2.03	2530	13	15.1	483	23	49.2	257
4	3.26	1630	14	17	445	24	55.4	241
5	4.12	1330	15	19.1	414	25	62.4	224
6	5.22	1090	16	21.5	386	26	70.2	208
7	6.61	896	17	24.2	363	27	79	194
8	8.38	745	18	27.3	339	28	88.9	181
9	9.43	679	19	30.7	321	29	100	171
10	10.6	621	20	34.6	304			

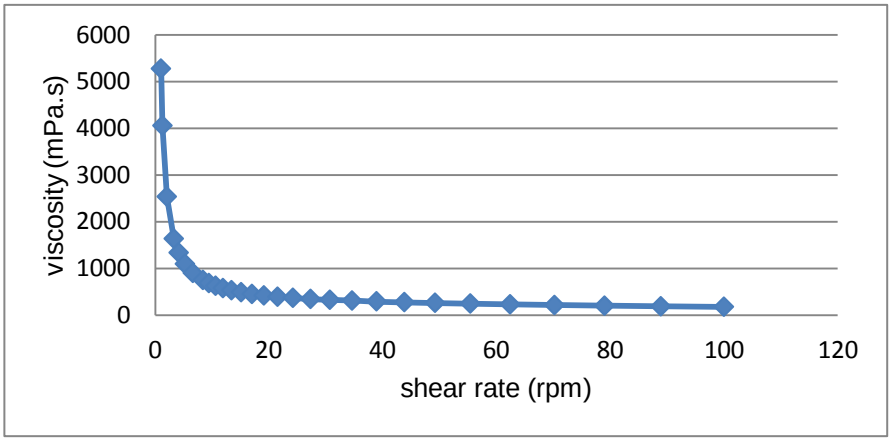

Figure A. 10: viscosity against shear rate for beta slurry at 20^0C

Table 19: viscosity measurement for beta slurry at 35^0C

S No.	Shear rate	Viscosity	S No.	Shear rate	Viscosity	S No.	Shear rate	Viscosity
	[1/min]	[mPa·s]		[1/min]	[mPa·s]		[1/min]	[mPa·s]
1	1	5230	11	10.6	610	21	34.6	264
2	1.27	3960	12	11.9	557	22	38.9	246
3	2.03	2500	13	13.4	509	23	43.8	230
4	3.26	1650	14	15.1	467	24	49.2	221
5	4.12	1340	15	17	427	25	55.4	207
6	5.22	1090	16	19.1	393	26	62.4	198
7	6.61	894	17	21.5	361	27	70.2	188
8	7.44	811	18	24.2	332	28	79	179
9	8.38	738	19	27.3	307	29	88.9	168
10	9.43	671	20	30.7	284	30	100	161

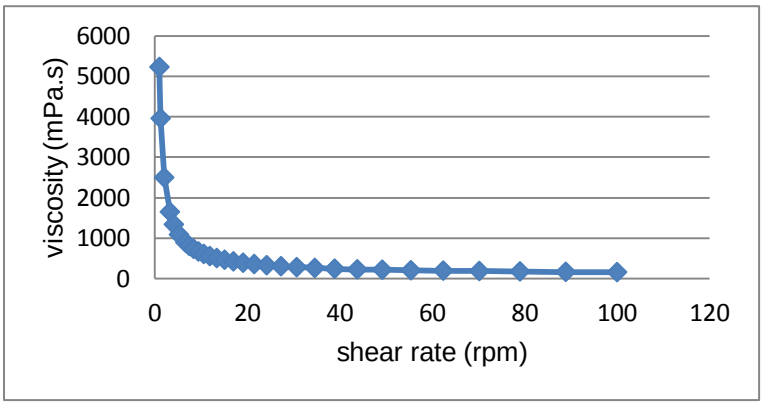

Figure A. 11: viscosity against shear rate for beta slurry at 35^0C

Table 20: viscosity measurement for beta slurry at 50^0C

S No.	Shear rate	Viscosity	S No.	Shear rate	Viscosity	S No.	Shear rate	Viscosity
	[1/min]	[mPa·s]		[1/min]	[mPa·s]		[1/min]	[mPa·s]
1	1	5570	11	10.6	636	21	34.6	260
2	1.27	4260	12	11.9	578	22	38.9	240
3	2.03	2600	13	13.4	526	23	43.8	220
4	3.26	1730	14	15.1	481	24	49.2	204
5	4.12	1410	15	17	438	25	55.4	186
6	5.22	1150	16	19.1	401	26	62.4	174
7	6.61	945	17	21.5	366	27	70.2	160
8	7.44	851	18	24.2	336	28	79	151
9	8.38	774	19	27.3	308	29	88.9	141
10	9.43	702	20	30.7	283	30	100	133

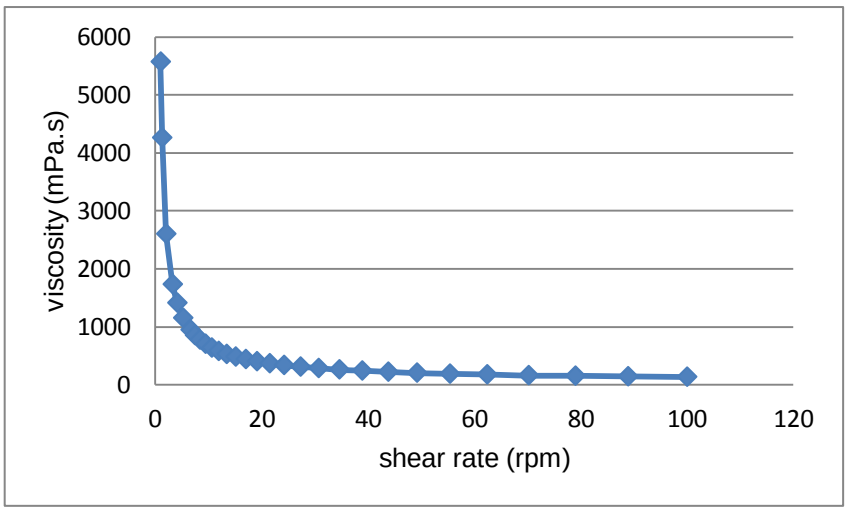

Figure A. 12: viscosity against shear rate for beta slurry at 50^0C

Table 21: viscosity measurement for theta slurry at 20^0C

S No.	Shear rate	Viscosity	S No.	Shear rate	Viscosity	S No.	Shear rate	Viscosity
	[1/min]	[mPa·s]		[1/min]	[mPa·s]		[1/min]	[mPa·s]
1	1	69000	11	9.43	8980	21	34.5	3700
2	1.13	60800	12	10.6	8280	22	38.9	3460
3	1.27	53000	13	13.4	6810	23	43.8	3310
4	2.04	36500	14	15.1	6370	24	49.2	3120
5	3.26	21300	15	17	5780	25	55.4	2950
6	4.13	17700	16	19.1	5240	26	62.4	2800
7	5.22	14400	17	21.5	4960	27	70.2	2630
8	6.61	11900	18	24.2	4560	28	78.9	2510
9	7.45	11100	19	27.3	4240	29	88.9	2360
10	8.38	10100	20	30.7	3890	30	100	2270

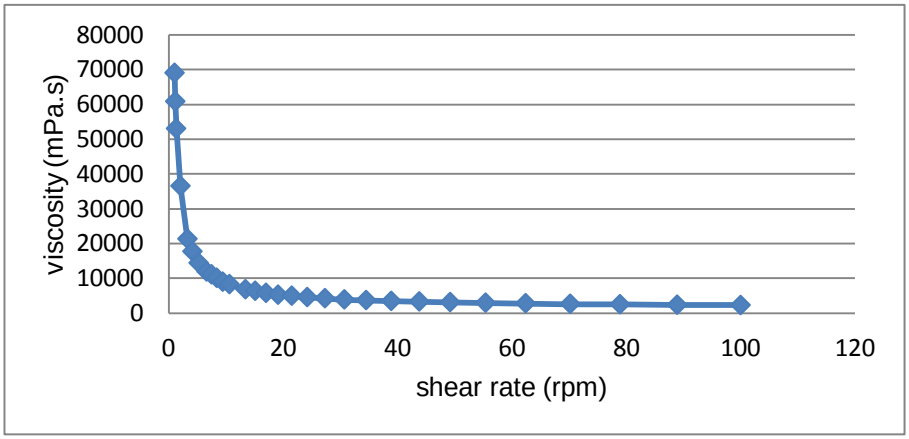

Figure A. 13: viscosity against shear rate for theta slurry at 20^0C

Table 22: viscosity measurement for theta slurry at 35^0C

S No.	Shear rate	Viscosity	S No.	Shear rate	Viscosity	S No.	Shear rate	Viscosity
	[1/min]	[mPa·s]		[1/min]	[mPa·s]		[1/min]	[mPa·s]
1	0.999	64700	11	9.42	8150	21	34.6	3050
2	1.12	57800	12	10.6	7350	22	38.9	2850
3	1.27	50400	13	11.9	6680	23	43.8	2690
4	2.03	36000	14	13.4	6130	24	49.2	2520
5	3.26	19200	15	15.1	5410	25	55.4	2370
6	4.12	16500	16	19.1	4710	26	62.4	2260
7	5.22	13400	17	21.5	4140	27	70.2	2130
8	6.62	11000	18	24.3	3930	28	79	2040
9	7.44	9630	19	27.3	3580	29	88.9	1950
10	8.38	8700	20	30.7	3330	30	100	1860

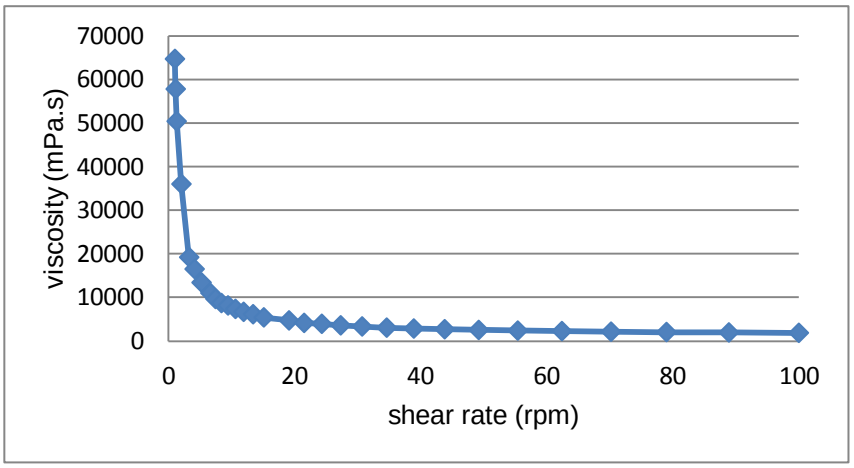

Figure A. 14: viscosity against shear rate for theta slurry at 35^{0}C

Table 23: viscosity measurement for theta slurry at 50^{0}C

S No.	Shear rate	Viscosity	S No.	Shear rate	Viscosity	S No.	Shear rate	Viscosity
	[1/min]	[mPa·s]		[1/min]	[mPa·s]		[1/min]	[mPa·s]
1	1	66300	12	9.43	7700	23	34.6	2890
2	1.13	86800	13	10.6	6960	24	38.9	2710
3	1.27	60900	14	11.9	6350	25	43.8	2530
4	2.03	36200	15	13.4	5640	26	49.2	2340
5	3.26	24000	16	15.1	5300	27	55.4	2190
6	4.12	16800	17	17	4760	28	62.3	2040
7	4.64	15200	18	19.2	4390	29	70.2	1940
8	5.23	12500	19	21.5	4000	30	79	1830
9	6.62	10100	20	24.2	3680	31	88.9	1730
10	7.44	9230	21	27.3	3390	32	100	1630
11	8.38	8530	22	30.7	3110			

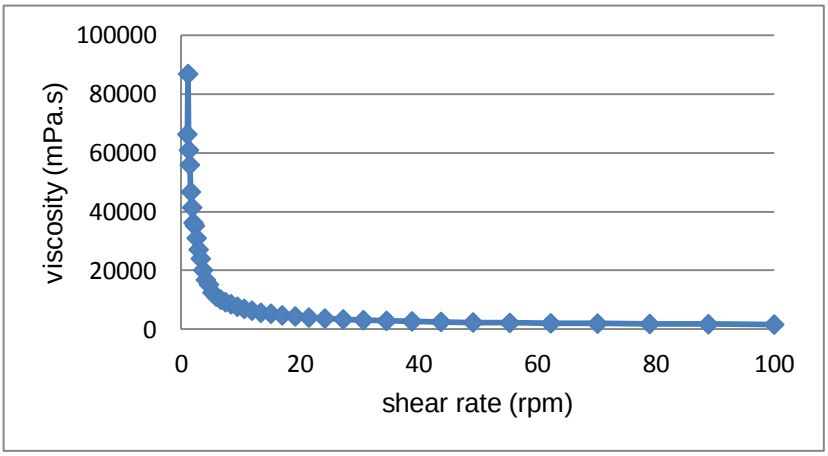

Figure A. 15: viscosity against shear rate for theta slurry at 50^{0}C

7.2 Appendix B: Sedimentation result

Big scale experiment

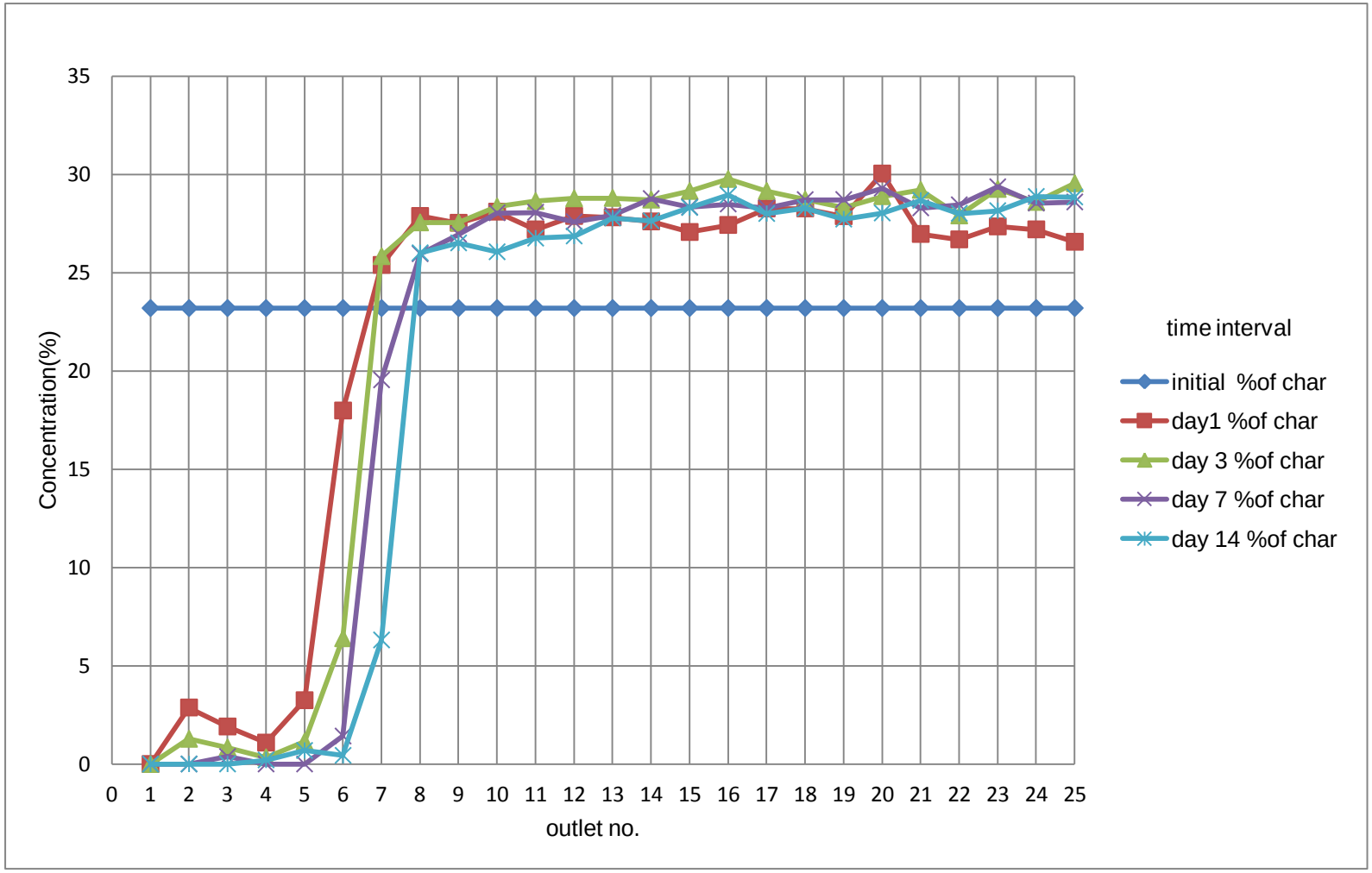

Figure A. 16: concentration at different outlets for alpha slurry in different time intervals

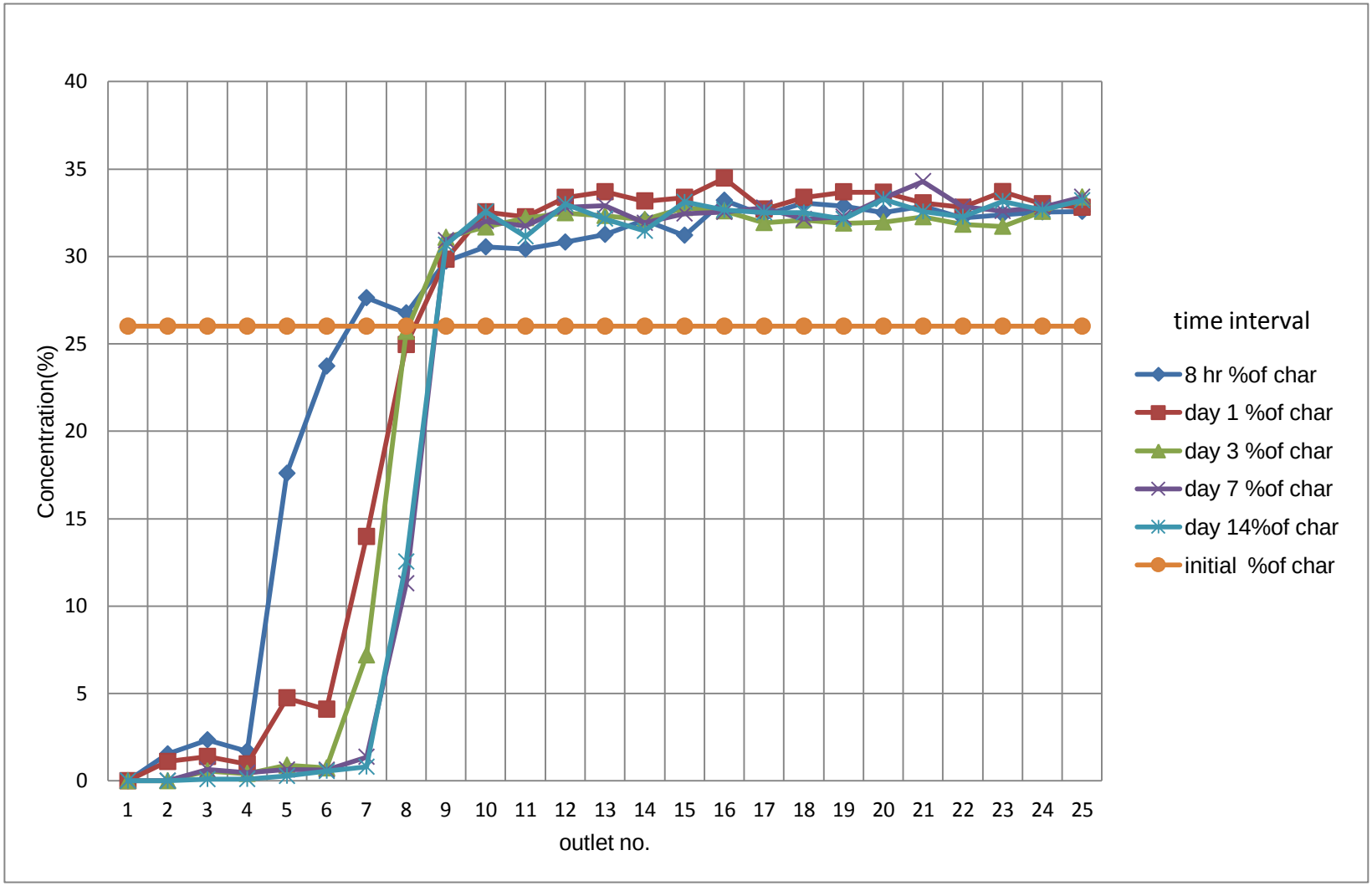

Figure A. 17: concentration at different outlets for beta slurry (full) in different time intervals

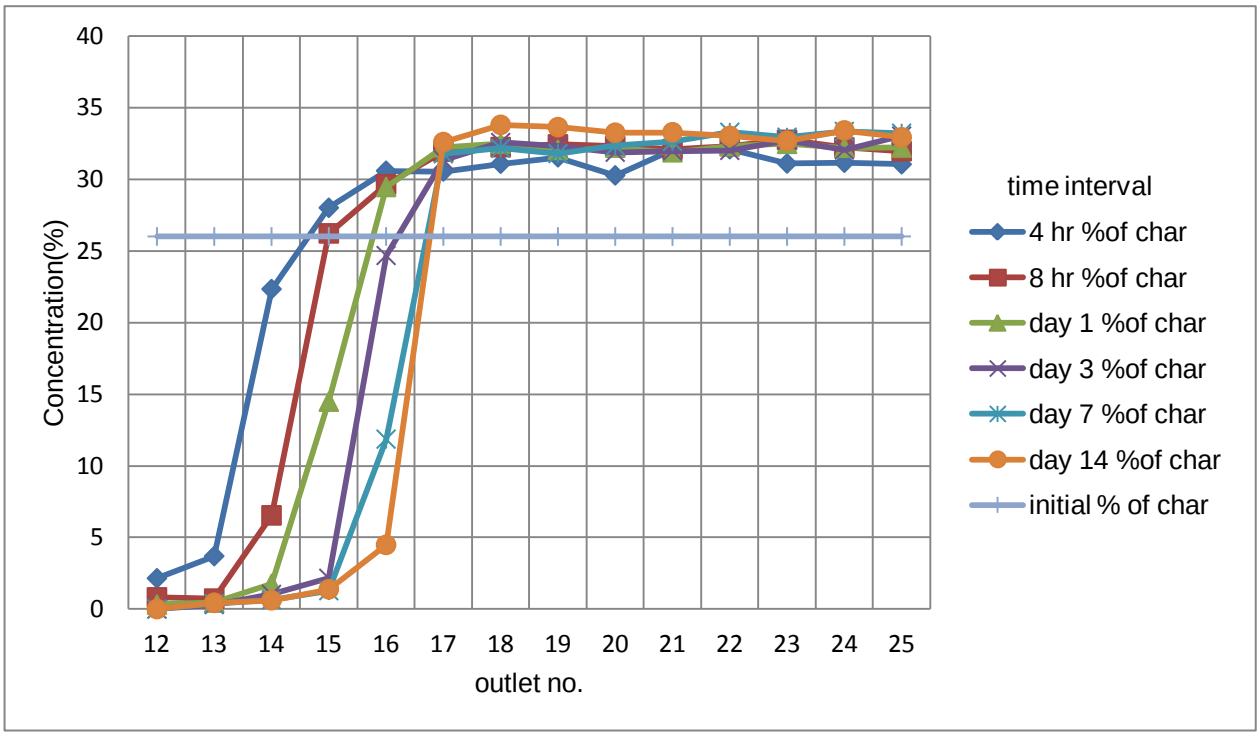

Figure A. 18:concentration at different outlets for beta slurry (half) in different time intervals

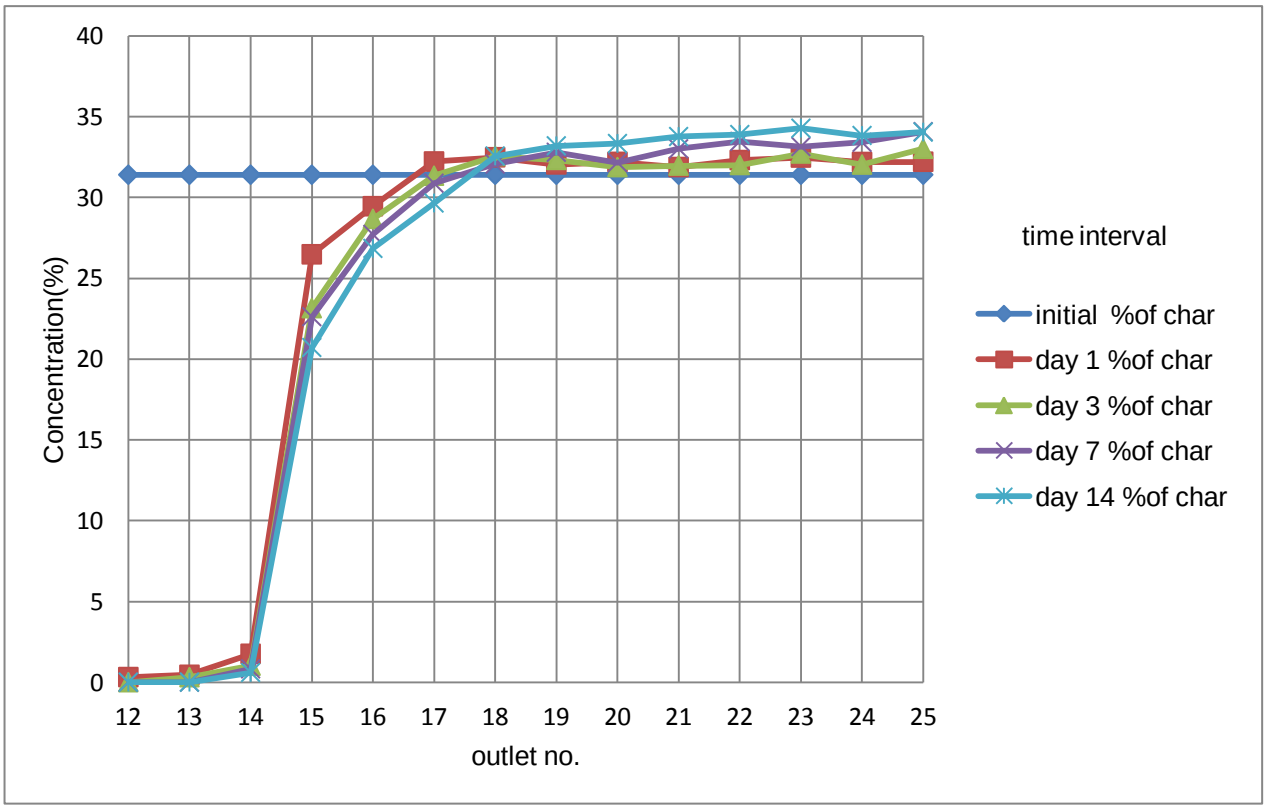

Figure A. 19: concentration at different outlets for theta slurry in different time intervals

Lab scale experiment

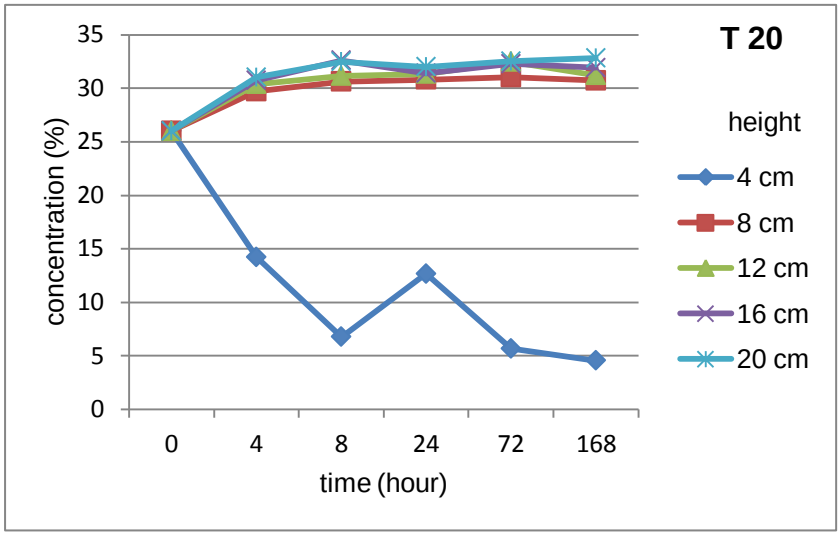

Figure A. 20: concentration against time intervals at different height for beta slurry in small cylinder at room temperature (20^0C)

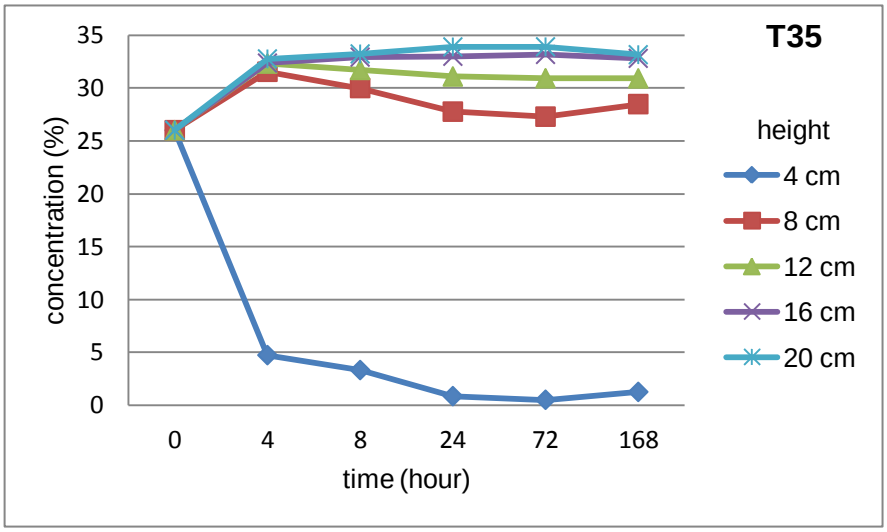

Figure A. 21: concentration against time intervals at different height for beta slurry in small cylinder at 35^0C

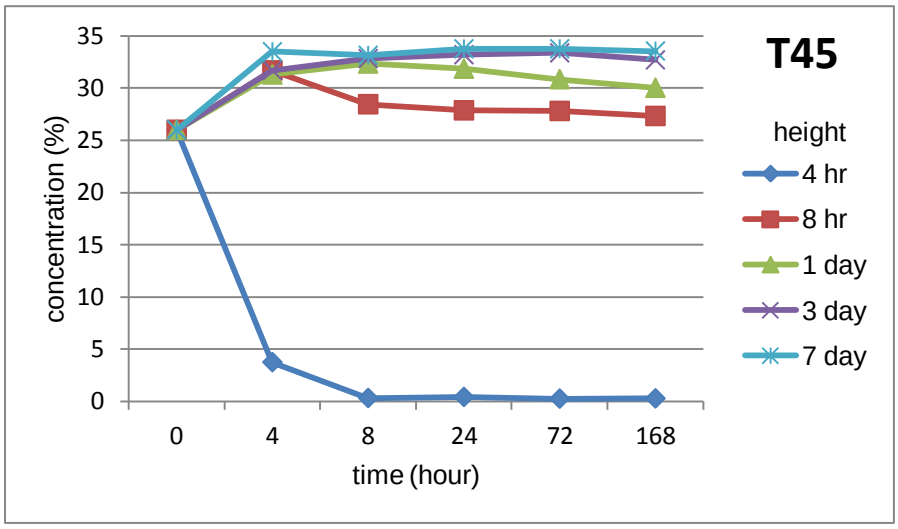

Figure A. 22: concentration against time intervals at different height for beta slurry in small cylinder at 45^0C